Rouse Chains with Excluded Volume Interactions: Linear Viscoelasticity

J. Ravi Prakash*
Department of Chemical Engineering,
Indian Institute of Technology, Madras, India 600 036

February 29, 2000

Abstract

Linear viscoelastic properties for a dilute polymer solution are predicted by modeling the solution as a suspension of non-interacting bead-spring chains. The present model, unlike the Rouse model, can describe the solution's rheological behavior even when the solvent quality is *good*, since *excluded volume* effects are explicitly taken into account through a narrow Gaussian repulsive potential between pairs of beads in a bead-spring chain. The use of the narrow Gaussian potential, which tends to the more commonly used δ-function repulsive potential in the limit of a *width* parameter d going to zero, enables the performance of Brownian dynamics simulations. The simulations results, which describe the exact behavior of the model, indicate that for chains of *arbitrary* but *finite* length, a δ-function potential leads to equilibrium and zero shear rate properties which are identical to the predicitions of the Rouse model. On the other hand, a non-zero value of d gives rise to a prediction of swelling at equilibrium, and an increase in zero shear rate properties relative to their Rouse model values. The use of a δ-function potential appears to be justified in the limit of infinite chain length. The exact simulation results are compared with those obtained with an approximate solution, which is based on the assumption that the non-equilibrium configurational distribution function is Gaussian. The Gaussian approximation is shown to be exact to first order in the strength of excluded volume interaction, and is used to explore long chain rheological properties by extrapolating results obtained numerically for finite chains, to the limit of infinite chain length.

*Present address: *Fachbereich Mathematik, Universität Kaiserslautern, D 67653 Germany*

1 Introduction

The simplest model, within the context of Polymer Kinetic Theory, to describe the rheological behavior of dilute polymer solutions is the Rouse model.[16] The Rouse model represents the macromolecule by a linear chain of identical beads connected by Hookean springs, and assumes that the solvent influences the motion of the beads by exerting a drag force and a Brownian force. While the Rouse model is able to explain the existence of viscoelasticity in polymer solutions by predicting a constant non-zero first normal stress difference in simple shear flow, it cannot predict several other features of dilute solution behavior, such as the existence of a nonzero second normal stress difference, the existence of shear rate dependent viscometric functions, or the correct molecular weight dependence of material functions. Over the past decade, considerable progress has been made by incorporating the effect of fluctuating hydrodynamic interaction into the Rouse model.[7,11,12,20,22] These models are able to predict the molecular weight dependence of the material functions accurately. They also predict a nonzero second normal stress difference, and shear rate dependent viscometric functions. However, since they neglect the existence of excluded volume interactions among parts of the polymer chain, they are strictly applicable only to *theta* solutions.

Recently, Prakash and Öttinger[13] examined the influence of excluded volume effects on the rheological behavior of dilute polymer solutions by representing the polymer molecule with a Hookean dumbbell model, and using a narrow Gaussian repulsive potential to describe the excluded volume interactions between the beads of the dumbbell. The narrow Gaussian potential tends to a δ-function potential in the limit of a parameter, d, that describes the width of the potential, going to zero. It can therefore be used to evaluate results obtained with the singular δ-function potential. It was shown by them that the use of a δ-function potential between the beads, which is commonly used in static theories for polymer solutions,[3,4,17] leads to no change in the equilibrium or dynamic properties of the dumbbell when compared to the case where no excluded volume interactions are taken into account. They also found that assuming that the non-equilibrium configurational distribution function is a Gaussian leads to very accurate predictions of viscometric functions in a certain range of parameter values. These results suggest that it would be worthwhile examining longer bead-spring chains. Firstly, it is interesting to see if the problem with the δ-function potential can be resolved when there are more beads in the bead-spring chain. Secondly, it is important to find out if the Gaussian approximation is accurate even for longer chains. If it is so, then it provides an alternative means—to renormalisation group theory[9,23]—of obtaining universal rheological properties. The purpose of this paper is to attempt to answer these questions, in the linear viscoelastic limit, by extending the methodology developed in the earlier paper to the case of bead-spring chains. The same issues, in the context of steady shear flows at finite shear rates, will be addressed in a subsequent paper.

As in the dumbbell paper, we confine our attention to excluded volume interactions alone, and neglect the presence of hydrodynamic interactions. This clearly

implies—since it is essential to include hydrodynamic interaction effects for a proper description of the dynamic behavior of dilute solutions—that the results of the present paper are not yet directly comparable with experiments. They represent a preliminary step in that direction. It is felt that the inclusion of hydrodynamic interaction would make the theory significantly more complex before the role of excluded volume interactions is properly understood. The aim of this work is to develop and carefully evaluate a systematic approximation procedure for excluded volume interactions, that might subsequently be useful in a combined theory of hydrodynamic interaction and excluded volume.

This paper is organized as follows. In the next section, the basic equations governing the dynamics of Rouse chains with excluded volume interactions are discussed. A retarded motion expansion for the stress tensor is derived in section 3, and exact expressions for the zero shear rate viscometric functions in simple shear flow are obtained. The implications of these results for a δ-function excluded volume potential are then discussed. In section 4, the Brownian dynamics simulation algorithm used in this work is described. Section 5 is devoted to the development of the Gaussian approximation for the configurational distribution function. Exact expressions for linear viscoelastic properties are derived through a codeformational memory-integral expansion. In section 6, a first order perturbation expansion in the strength of the excluded volume interaction—in an arbitrary number of space dimensions—is carried out. This proves to be very helpful in understanding the nature of the Gaussian approximation. Renormalisation of the equilibrium end-to-end vector is also considered in this section, in order to elucidate the role of the parameter d in the long chain limit. The results of the various exact and approximate treatments are compared and discussed in section 7, and the main conclusions of the paper are summarized in section 8.

2 Basic Equations

The instantaneous configuration of a linear bead-spring chain, which consists of N beads connected together by $(N-1)$ Hookean springs, is specified by the bead position vectors $\boldsymbol{r}_\nu$, $\nu = 1, 2, \ldots, N$, in a laboratory-fixed coordinate system. The Newtonian solvent, in which the chain is suspended, is assumed to have a homogeneous velocity field—that is, at position $\boldsymbol{r}$ and time t, the velocity is given by $\boldsymbol{v}(\boldsymbol{r}, t) = \boldsymbol{v}_0 + \boldsymbol{\kappa}(t) \cdot \boldsymbol{r}$, where $\boldsymbol{v}_0$ is a constant vector and $\boldsymbol{\kappa}(t)$ is a traceless tensor.

The microscopic picture of the intra-molecular forces within the bead-spring chain is one in which the presence of excluded volume interactions between the beads causes the chain to swell, while on the other hand, the entropic retractive force of the springs draws the beads together and opposes the excluded volume force. This is modeled by writing the potential energy ϕ of the bead-spring chain as a sum of the potential energy of the springs S, and the potential energy due to excluded volume interactions E. The potential energy S is the sum of the potential

energies of all the springs in the chain, and is given by,

$$S = \frac{1}{2} H \sum_{i=1}^{N-1} \boldsymbol{Q}_i \cdot \boldsymbol{Q}_i \tag{1}$$

where, H is the spring constant, and $\boldsymbol{Q}_i = \boldsymbol{r}_{i+1} - \boldsymbol{r}_i$, is the *bead connector* vector between the beads i and $i+1$. The excluded volume potential energy E is found by summing the interaction energy over all pairs of beads μ and ν,

$$E = \frac{1}{2} \sum_{\substack{\mu,\nu=1 \\ \mu \neq \nu}}^{N} E\left(\boldsymbol{r}_\nu - \boldsymbol{r}_\mu\right) \tag{2}$$

where, $E\left(\boldsymbol{r}_\nu - \boldsymbol{r}_\mu\right)$ is a short-range function. It is usually assumed to be a δ-function potential in static theories for polymer solutions,

$$E\left(\boldsymbol{r}_\nu - \boldsymbol{r}_\mu\right) = v\, k_{\mathrm{B}} T\, \delta\left(\boldsymbol{r}_\nu - \boldsymbol{r}_\mu\right) \tag{3}$$

where, v is the excluded volume parameter (with dimensions of volume), k_{B} is Boltzmann's constant, and T is the absolute temperature. In this work, we regularise the δ-function potential, and assume that $E\left(\boldsymbol{r}_\nu - \boldsymbol{r}_\mu\right)$ is given by a narrow Gaussian potential,

$$E\left(\boldsymbol{r}_\nu - \boldsymbol{r}_\mu\right) = \frac{v\, k_{\mathrm{B}} T}{\left[2\pi \tilde{d}^2\right]^{\frac{3}{2}}} \exp\left(-\frac{1}{2} \frac{\boldsymbol{r}_{\nu\mu}^2}{\tilde{d}^2}\right) \tag{4}$$

where, $\tilde{d}$ is a parameter that describes the width of the potential (it represents, in some sense, the *extent* of excluded volume interactions), and $\boldsymbol{r}_{\nu\mu} = \boldsymbol{r}_\nu - \boldsymbol{r}_\mu$, is the vector between beads μ and ν. In the limit $\tilde{d}$ tending to zero, the narrow Gaussian potential becomes a δ-function potential.

The *intra-molecular* force on a bead ν, $\boldsymbol{F}_\nu^{(\phi)} = -(\partial\phi/\partial\boldsymbol{r}_\nu)$, can consequently be written as, $\boldsymbol{F}_\nu^{(\phi)} = \boldsymbol{F}_\nu^{(S)} + \boldsymbol{F}_\nu^{(E)}$, where,

$$\boldsymbol{F}_\nu^{(S)} = -H \sum_{k=1}^{N-1} \overline{B}_{k\nu}\, \boldsymbol{Q}_k \tag{5}$$

$$\boldsymbol{F}_\nu^{(E)} = -\sum_{\substack{\mu=1 \\ \mu \neq \nu}}^{N} \frac{\partial}{\partial \boldsymbol{r}_\nu} E\left(\boldsymbol{r}_\nu - \boldsymbol{r}_\mu\right) \tag{6}$$

In equation (5), $\overline{B}_{k\nu}$ is an $(N-1) \times N$ matrix defined by, $\overline{B}_{k\nu} = \delta_{k+1,\,\nu} - \delta_{k\nu}$, with $\delta_{k\nu}$ denoting the Kronecker delta.

For homogeneous flows, the internal configurations of the bead-spring chain are expected to be independent of the location of the centre of mass. Consequently, it is assumed that the configurational distribution function ψ depends only on the $(N-1)$ bead connector vectors $\boldsymbol{Q}_k$. The diffusion equation that governs $\psi\left(\boldsymbol{Q}_1, \ldots, \boldsymbol{Q}_{N-1}, t\right)$, for a system with an intra-molecular potential energy ϕ as described above, can then

be shown to be given by,

$$\frac{\partial \psi}{\partial t} = - \sum_{j=1}^{N-1} \frac{\partial}{\partial \boldsymbol{Q}_j} \cdot \left(\boldsymbol{\kappa} \cdot \boldsymbol{Q}_j - \frac{H}{\zeta} \sum_{k=1}^{N-1} A_{jk} \boldsymbol{Q}_k + \frac{1}{\zeta} \sum_{\nu=1}^{N} \overline{B}_{j\nu} \boldsymbol{F}_{\nu}^{(E)} \right) \psi + \frac{k_{\mathrm{B}} T}{\zeta} \sum_{j,\,k=1}^{N-1} A_{jk} \frac{\partial}{\partial \boldsymbol{Q}_j} \cdot \frac{\partial \psi}{\partial \boldsymbol{Q}_k} \tag{7}$$

where, ζ is the bead friction coefficient (which, for spherical beads with radius a, in a solvent with viscosity η_s, is given by the Stokes expression: $\zeta = 6\pi\eta_s a$), and A_{jk} is the Rouse matrix,

$$A_{jk} = \sum_{\nu=1}^{N} \overline{B}_{j\nu} \overline{B}_{k\nu} = \begin{cases} 2 & \text{for } |j-k| = 0, \\ -1 & \text{for } |j-k| = 1, \\ 0 & \text{otherwise} \end{cases} \tag{8}$$

The time evolution of the average of any arbitrary quantity, carried out with the configurational distribution function ψ, can be obtained from the diffusion equation. In particular, by multiplying equation (7) by $\boldsymbol{Q}_j \boldsymbol{Q}_k$, and integrating over all configurations, the following time evolution equation for the second moments of the bead connector vectors is obtained,

$$\frac{d}{dt} \langle \boldsymbol{Q}_j \boldsymbol{Q}_k \rangle = \boldsymbol{\kappa} \cdot \langle \boldsymbol{Q}_j \boldsymbol{Q}_k \rangle + \langle \boldsymbol{Q}_j \boldsymbol{Q}_k \rangle \cdot \boldsymbol{\kappa}^T + \frac{2 k_{\mathrm{B}} T}{\zeta} A_{jk} \, \boldsymbol{1} - \frac{H}{\zeta} \sum_{m=1}^{N-1} \left\{ \langle \boldsymbol{Q}_j \boldsymbol{Q}_m \rangle A_{mk} + A_{jm} \langle \boldsymbol{Q}_m \boldsymbol{Q}_k \rangle \right\} + \boldsymbol{Y}_{jk} \tag{9}$$

where, $\boldsymbol{1}$ is the unit tensor, and,

$$\boldsymbol{Y}_{jk} = \frac{1}{\zeta} \sum_{\mu=1}^{N} \left\{ \langle \boldsymbol{Q}_j \boldsymbol{F}_{\mu}^{(E)} \rangle \overline{B}_{k\mu} + \overline{B}_{j\mu} \langle \boldsymbol{F}_{\mu}^{(E)} \boldsymbol{Q}_k \rangle \right\} \tag{10}$$

The term $\boldsymbol{Y}_{jk}$, which arises due to the presence of excluded volume interactions, does not appear in the second moment equation for the Rouse model. Due to this term, which in general involves higher order moments, equation (9), is not a closed equation for $\langle \boldsymbol{Q}_j \boldsymbol{Q}_k \rangle$. As will be discussed in greater detail in the section on the Gaussian approximation, finding an approximate solution for the present model revolves around making equation (9) a closed equation for the second moments.

The polymer contribution to the stress tensor—for models with arbitrary intramolecular potential forces but no internal constraints—is given by the *Kramers* expression,[2]

$$\boldsymbol{\tau}^p = -n_{\mathrm{p}} H \sum_{k=1}^{N-1} \langle \boldsymbol{Q}_k \boldsymbol{Q}_k \rangle + \boldsymbol{Z} + (N-1)\, n_{\mathrm{p}} k_{\mathrm{B}} T \, \boldsymbol{1} \tag{11}$$

where,

$$\boldsymbol{Z} = n_{\mathrm{p}} \sum_{\nu=1}^{N} \sum_{k=1}^{N-1} B_{\nu k} \langle \boldsymbol{Q}_k \boldsymbol{F}_{\nu}^{(E)} \rangle \tag{12}$$

Here, $n_{\rm p}$ is the number density of polymers, and $B_{\nu k}$ is a $N \times (N-1)$ matrix defined by, $B_{\nu k} = k/N - \Theta\,(k-\nu)$, with $\Theta\,(k-\nu)$ denoting a Heaviside step function.

It is clear from equation (11) that there are two reasons why the presence of excluded volume interactions leads to a stress tensor that is different from that obtained in the Rouse model. Firstly, there is an additional term represented by $\boldsymbol{Z}$ which is the *direct* influence of excluded volume effects. Secondly, there is an *indirect* influence due to a change in the contribution of the term $\sum_{k=1}^{N-1} \langle \boldsymbol{Q}_k \boldsymbol{Q}_k \rangle$, relative to its contribution in the Rouse case.

All the rheological properties of interest can be obtained once the stress tensor in equation (11) is evaluated. In the next section, a retarded motion expansion for the stress tensor is derived.

3 Retarded Motion Expansion

A retarded motion expansion for the stress tensor can be obtained by extending the derivation carried out previously for the dumbbell model[13] to the case of bead-spring chains. The dumbbell model derivation was, in turn, an adaptation of a similar development for the FENE dumbbell model.[2] The argument in all these cases rests basically on seeking a solution of the diffusion equation, equation (7), of the following form,

$$\psi(\boldsymbol{Q}_1, \ldots, \boldsymbol{Q}_{N-1}, t) = \psi_{\rm eq}(\boldsymbol{Q}_1, \ldots, \boldsymbol{Q}_{N-1})\, \phi_{\rm fl}\,(\boldsymbol{Q}_1, \ldots, \boldsymbol{Q}_{N-1}, t) \tag{13}$$

where, $\psi_{\rm eq}$ is the equilibrium distribution function given by,

$$\psi_{\rm eq}(\boldsymbol{Q}_1, \ldots, \boldsymbol{Q}_{N-1}) = \mathcal{N}_{\rm eq}\, e^{-\phi/k_{\rm B}T} \tag{14}$$

with $\mathcal{N}_{\rm eq}$ denoting the normalization constant, and $\phi_{\rm fl}$ is the correction to $\psi_{\rm eq}$ due to flow—appropriately termed the flow contribution.

The governing partial differential equation for $\phi_{\rm fl}\,(\boldsymbol{Q}_1, \ldots, \boldsymbol{Q}_{N-1}, t)$ can be obtained by substituting equation (13) into the diffusion equation (7). It turns out that, regardless of the form of the excluded volume potential, at steady state, an exact solution to this partial differential equation can be found for all homogeneous *potential* flows. For more general homogeneous flows, however, one can only obtain a perturbative solution of the form,

$$\phi_{\rm fl}\,(\boldsymbol{Q}_1, \ldots, \boldsymbol{Q}_{N-1}, t) = 1 + \phi_1 + \phi_2 + \phi_3 + \ldots \tag{15}$$

where ϕ_k is of order k in the velocity gradient.

Partial differential equations governing each of the ϕ_k may be derived by substituting equation (15) into the partial differential equation for $\phi_{\rm fl}$ and equating terms of like order. The forms of the functions ϕ_k can then be guessed by requiring that they fulfill certain conditions.[2] In the present instance, we only find the form of ϕ_1, since we are interested in the stress tensor correct only to second order in the

velocity gradient. One can show that,

$$\phi_1 = \frac{\zeta}{4k_{\rm B}T} \sum_{m,n=1}^{N-1} C_{mn}\, \boldsymbol{Q}_m \cdot \dot{\boldsymbol{\gamma}} \cdot \boldsymbol{Q}_n \tag{16}$$

where, $\dot{\boldsymbol{\gamma}}$ is the rate of strain tensor, $\dot{\boldsymbol{\gamma}} = \nabla \boldsymbol{v} + \nabla \boldsymbol{v}^T$, and C_{mn} is the Kramers matrix. The Kramers matrix is the inverse of the Rouse matrix, and is defined by,

$$C_{mn} = \sum_{\nu=1}^{N} B_{\nu m} B_{\nu n} = \min(m,n) - mn/N \tag{17}$$

In order to proceed further, we need to show that the present model satisfies the Giesekus expression for the stress tensor.[2] Upon multiplying equation (7) with $\sum_{m,n=1}^{N-1} C_{mn}\, \boldsymbol{Q}_m \boldsymbol{Q}_n$, and integrating over all configurations, we can show that,

$$\begin{aligned} &\frac{d}{dt} \sum_{m,n=1}^{N-1} \langle C_{mn}\, \boldsymbol{Q}_m \boldsymbol{Q}_n \rangle - \sum_{m,n=1}^{N-1} C_{mn} \left[\boldsymbol{\kappa} \cdot \langle \boldsymbol{Q}_m \boldsymbol{Q}_n \rangle + \langle \boldsymbol{Q}_m \boldsymbol{Q}_n \rangle \cdot \boldsymbol{\kappa}^T \right] \\ &= \frac{2k_{\rm B}T}{\zeta} (N-1)\, \boldsymbol{1} - \frac{2H}{\zeta} \sum_{m=1}^{N-1} \langle \boldsymbol{Q}_m \boldsymbol{Q}_m \rangle + \frac{2}{\zeta} \sum_{\nu=1}^{N} \sum_{m=1}^{N-1} B_{\nu m} \langle \boldsymbol{Q}_m \boldsymbol{F}_{\nu}^{(E)} \rangle \end{aligned} \tag{18}$$

On combining this equation with equation (11) for the stress tensor, it is straight forward to see that the Giesekus expression is indeed satisfied. At steady state the Giesekus expression reduces to,

$$\boldsymbol{\tau}^p = -\frac{n_{\rm p}\, \zeta}{2} \sum_{m,n=1}^{N-1} C_{mn} \left\{ \boldsymbol{\kappa} \cdot \langle \boldsymbol{Q}_m \boldsymbol{Q}_n \rangle + \langle \boldsymbol{Q}_m \boldsymbol{Q}_n \rangle \cdot \boldsymbol{\kappa}^T \right\} \tag{19}$$

Clearly, the stress tensor at steady state can be found once the average $\langle \boldsymbol{Q}_m \boldsymbol{Q}_n \rangle$ is evaluated. This can be done, correct to first order in velocity gradients, by using the power series expansion (15) for $\phi_{\rm fl}$, with the specific form for ϕ_1 in equation (16). The following retarded motion expansion for the stress tensor, correct to second order in velocity gradients and valid for arbitrary homogeneous flows, is then obtained,

$$\begin{aligned} \boldsymbol{\tau}^p &= -\frac{n_{\rm p}\, \zeta}{2} \sum_{m,n=1}^{N-1} C_{mn} \left[\boldsymbol{\kappa} \cdot \langle \boldsymbol{Q}_m \boldsymbol{Q}_n \rangle_{\rm eq} + \langle \boldsymbol{Q}_m \boldsymbol{Q}_n \rangle_{\rm eq} \cdot \boldsymbol{\kappa}^T \right] \\ &- \frac{n_{\rm p}\, \zeta^2}{8k_{\rm B}T} \sum_{m,n=1}^{N-1} \sum_{j,k=1}^{N-1} C_{mn} C_{jk} \Big[\boldsymbol{\kappa} \cdot \langle \boldsymbol{Q}_m \boldsymbol{Q}_n (\boldsymbol{Q}_j \cdot \dot{\boldsymbol{\gamma}} \cdot \boldsymbol{Q}_k) \rangle_{\rm eq} \\ &+ \langle (\boldsymbol{Q}_j \cdot \dot{\boldsymbol{\gamma}} \cdot \boldsymbol{Q}_k) \boldsymbol{Q}_m \boldsymbol{Q}_n \rangle_{\rm eq} \cdot \boldsymbol{\kappa}^T \Big] + \ldots \end{aligned} \tag{20}$$

where, $\langle X \rangle_{\rm eq}$ denotes the average of any arbitrary quantity X with the equilibrium distribution function $\psi_{\rm eq}$.

One can see clearly from equation (20) that rheological properties, at small values of the velocity gradient, can be obtained by merely evaluating equilibrium averages. The special case of steady simple shear flow in the limit of zero shear rate is considered below.

3.1 Zero Shear Rate Viscometric Functions

Steady simple shear flows are described by a tensor $\boldsymbol{\kappa}$ which has the following matrix representation in the laboratory-fixed coordinate system,

$$\boldsymbol{\kappa} = \dot{\gamma} \begin{pmatrix} 0 & 1 & 0 \\ 0 & 0 & 0 \\ 0 & 0 & 0 \end{pmatrix} \tag{21}$$

where $\dot{\gamma}$ is the constant shear rate.

The three independent material functions used to characterize such flows are the viscosity, η_p, and the first and second normal stress difference coefficients, Ψ_1 and Ψ_2, respectively. These functions are defined by the following relations,[1]

$$\tau^p_{xy} = -\dot{\gamma}\,\eta_p\,; \qquad \tau^p_{xx} - \tau^p_{yy} = -\dot{\gamma}^2\,\Psi_1\,; \qquad \tau^p_{yy} - \tau^p_{zz} = -\dot{\gamma}^2\,\Psi_2 \tag{22}$$

The components of the stress tensor in simple shear flow, for small values of the shear rate $\dot{\gamma}$, can be found by substituting equation (21) for the rate of strain tensor, into equation (20). This leads to,

$$\begin{aligned} \tau^p_{xy} &= -\frac{n_{\rm p}\,\zeta\,\dot{\gamma}}{2} \sum_{m,n=1}^{N-1} C_{mn}\,\langle Y_m Y_n\rangle_{\rm eq} - \frac{n_{\rm p}\,\zeta^2\,\dot{\gamma}^2}{4k_{\rm B}T} \sum_{m,n=1}^{N-1}\sum_{p,q=1}^{N-1} C_{mn}C_{pq}\langle Y_m Y_n X_p Y_q\rangle_{\rm eq} \\ \tau^p_{xx} &= -n_{\rm p}\,\zeta\,\dot{\gamma} \sum_{m,n=1}^{N-1} C_{mn}\,\langle X_m Y_n\rangle_{\rm eq} - \frac{n_{\rm p}\,\zeta^2\,\dot{\gamma}^2}{2k_{\rm B}T} \sum_{m,n=1}^{N-1}\sum_{p,q=1}^{N-1} C_{mn}C_{pq}\langle X_m Y_n X_p Y_q\rangle_{\rm eq} \\ \tau^p_{yy} &= \tau^p_{zz} = 0 \end{aligned} \tag{23}$$

where, (X_m, Y_m, Z_m) are the Cartesian components of the bead connector vector $\boldsymbol{Q}_m$.

Using the symmetry property of the potential energy ϕ, which remains unchanged when the sign of the Y_k component of all the bead connector vectors $\boldsymbol{Q}_k; k = 1, 2, \ldots, (N-1)$, is reversed, we can show that, $\langle X_m Y_n\rangle_{\rm eq} = 0$. From the definitions of the viscometric functions in equation (22), it is straight forward to show that, in the limit of zero shear rate, the following exact expressions for the zero shear rate viscometric functions are obtained.

$$\eta_{p,0} = \frac{n_{\rm p}\,\zeta}{6} \sum_{m,n=1}^{N-1} C_{mn}\,\langle \boldsymbol{Q}_m \cdot \boldsymbol{Q}_n\rangle_{\rm eq} \tag{24}$$

$$\Psi_{1,0} = \frac{n_{\rm p}\,\zeta^2}{2k_{\rm B}T} \sum_{m,n=1}^{N-1}\sum_{p,q=1}^{N-1} C_{mn}C_{pq}\,\langle X_m Y_n X_p Y_q\rangle_{\rm eq} \tag{25}$$

$$\Psi_{2,0} = 0 \tag{26}$$

In order to derive equation (24), we have used the fact that, since ϕ is the same function of X_p, Y_p, and Z_p for all p, $\langle X_p X_q\rangle_{\rm eq} = \langle Y_p Y_q\rangle_{\rm eq} = \langle Z_p Z_q\rangle_{\rm eq}$. Equation (26) indicates that the inclusion of excluded volume interactions alone is not sufficient

to lead to the prediction of a non-zero second normal stress difference. The proper inclusion of hydrodynamic interaction is required.

It is interesting to note, by making use of equation (24), that the mean square radius of gyration at equilibrium, which is defined as,[2]

$$\langle R_g^2 \rangle_{\rm eq} = \frac{1}{N} \sum_{\nu=1}^{N} \int d\boldsymbol{Q}_1 d\boldsymbol{Q}_2 \ldots d\boldsymbol{Q}_{N-1} \, (\boldsymbol{r}_\nu - \boldsymbol{r}_c) \cdot (\boldsymbol{r}_\nu - \boldsymbol{r}_c) \, \psi_{\rm eq} \tag{27}$$

(where, $\boldsymbol{r}_c$ is the position of the center of mass), is related to the zero shear rate viscosity by,

$$\eta_{p,0} = \frac{n_{\rm p} \, \zeta}{6} \, N \, \langle R_g^2 \rangle_{\rm eq} \tag{28}$$

An alternative expression for the zero shear rate viscosity, which will prove very useful subsequently, can also be obtained from equation (24),

$$\eta_{p,0} = \frac{n_{\rm p} \, \zeta}{12N} \sum_{\nu,\mu=1}^{N} \langle \boldsymbol{r}_{\nu\mu}^2 \rangle_{\rm eq} \tag{29}$$

In order to derive equations (28) and (29), equations which relate the bead connector vector coordinates to bead position vector coordinates, summarized for example, in Chapter 11 and Table 15.1-1 of Chapter 15 of the text book by Bird et al.,[2] have been used.

The evaluation of the equilibrium averages in equations (25) and (29), for various values of the parameters in the narrow Gaussian potential, and for various chain lengths N, have been carried out here with the help of Brownian dynamics simulations. More details of these simulations are given subsequently. In the special case of the extent of excluded volume interactions $\tilde{d}$ going to zero or infinity, we had shown earlier for a Hookean dumbbell model that the values of $\eta_{p,0}$ and $\Psi_{1,0}$ remain unchanged from the values that they have in the absence of excluded volume interactions.[13] In the next section, we consider the same limits for the more general case of bead-spring chains of arbitrary (but finite) length.

3.2 The Limits $\tilde{d} \to 0$ and $\tilde{d} \to \infty$

The average in equation (29) can be evaluated with the equilibrium distribution function $\psi_{\rm eq}(\boldsymbol{Q}_1, \ldots, \boldsymbol{Q}_{N-1})$, or equivalently, with the equilibrium distribution function $P_{\rm eq}(\boldsymbol{r}_{\nu\mu})$, which is a contracted distribution function for each vector $\boldsymbol{r}_{\nu\mu}$, and which is defined by,

$$P_{\rm eq}(\boldsymbol{r}_{\nu\mu}) = \int d\boldsymbol{Q}_1 d\boldsymbol{Q}_2 \ldots d\boldsymbol{Q}_{N-1} \, \delta \left(\boldsymbol{r}_{\nu\mu} - \sum_{j=\mu}^{\nu-1} \boldsymbol{Q}_j \right) \psi_{\rm eq} \tag{30}$$

We have assumed here, without loss of generality, that $\nu > \mu$.

In the Rouse model, as is well known, the equilibrium distribution function is Gaussian,

$$\psi^R_{\rm eq}\,(\,\boldsymbol{Q}_1,\ldots,\,\boldsymbol{Q}_{N-1}\,) = \prod_{j=1}^{N-1}\left(\frac{H}{2\pi k_{\rm B}T}\right)^{3/2}\exp\left(-\frac{H}{2\,k_{\rm B}T}\,\boldsymbol{Q}_j\cdot\boldsymbol{Q}_j\right) \tag{31}$$

A superscript or subscript 'R' on any quantity will henceforth indicate a quantity defined or evaluated in the Rouse model. The distribution function $P^R_{\rm eq}(\boldsymbol{r}_{\nu\mu})$ can then be evaluated, by substituting equation (31) and the Fourier representation of a δ-function, into equation (30),[2]

$$P^R_{\rm eq}\,(\boldsymbol{r}_{\nu\mu}) = \left(\frac{H}{2\pi k_{\rm B}T\,|\nu-\mu|}\right)^{3/2}\exp\left(-\frac{H}{2\,|\nu-\mu|\,k_{\rm B}T}\,\boldsymbol{r}^2_{\nu\mu}\right) \tag{32}$$

The absolute value $|\nu-\mu|$ indicates that this expression is valid regardless of whether ν or μ is greater. This is another well known result of the Rouse model, namely, at equilibrium, the vector $\boldsymbol{r}_{\nu\mu}$ between any two beads μ and ν, also obeys a Gaussian distribution.

A similar procedure can be adopted to evaluate $P_{\rm eq}(\boldsymbol{r}_{\nu\mu})$, in the presence of excluded volume interactions, by substituting equation (14) and the Fourier representation of a δ-function, into equation (30). We show rigorously in appendix A that,

$$\lim_{\substack{\tilde{d}\to 0\\ \text{or, }\tilde{d}\to\infty}} P_{\rm eq}(\boldsymbol{r}_{\nu\mu}) = P^R_{\rm eq}\,(\boldsymbol{r}_{\nu\mu}) \tag{33}$$

As a result, all averages evaluated with $P_{\rm eq}(\boldsymbol{r}_{\nu\mu})$, tend, in the limit $\tilde{d}\to 0$ or $\tilde{d}\to\infty$, to averages evaluated with $P^R_{\rm eq}\,(\boldsymbol{r}_{\nu\mu})$. Consequently, $\lim_{\substack{\tilde{d}\to 0\\ \text{or, }\tilde{d}\to\infty}} \langle\boldsymbol{r}^2_{\nu\mu}\rangle_{\rm eq} = \langle\boldsymbol{r}^2_{\nu\mu}\rangle^R_{\rm eq}$, and from equation (29),

$$\lim_{\substack{\tilde{d}\to 0\\ \text{or, }\tilde{d}\to\infty}} \eta_{p,0} = \eta^R_{p,0} \tag{34}$$

Thus, the polymer contribution to the viscosities in the limit of zero shear rate, for chains of arbitrary (but finite) length, in (i) the presence of δ-function excluded volume interactions, and (ii) the absence of excluded volume interactions (the Rouse model), are identical to each other. Brownian dynamics simulations, details of which are given in the section below, indicate that this is also true for the first normal stress difference coefficients.

4 Brownian Dynamics Simulations

The equilibrium averages in equations (25) and (29), as mentioned above, can be evaluated with the help of Brownian dynamics simulations. As a result, exact numerical predictions of the zero shear rate viscometric functions can be obtained. Brownian dynamics simulations basically involve the numerical solution of the Ito

stochastic differential equation that corresponds to the diffusion equation, equation (7). Using standard methods[10] to transcribe a Fokker-Planck equation to a stochastic differential equation, one can show that equation (7) is equivalent to the following system of $(N-1)$ stochastic differential equations for the connector vectors $\boldsymbol{Q}_j$,

$$d\boldsymbol{Q}_j = \left\{ \boldsymbol{\kappa} \cdot \boldsymbol{Q}_j - \frac{1}{\zeta} \sum_{k=1}^{N-1} A_{jk} \frac{\partial \phi}{\partial \boldsymbol{Q}_k} \right\} dt + \sum_{\nu=1}^{N} \sqrt{\frac{2k_{\mathrm{B}}T}{\zeta}}\, \overline{B}_{j\nu}\, d\boldsymbol{W}_\nu \tag{35}$$

where, $\boldsymbol{W}_\nu$ is a $3N$ dimensional Wiener process.

A second order predictor-corrector algorithm with time-step extrapolation[10] was used for the numerical solution of equation (35). Steady-state expectations at equilibrium were obtained by setting $\boldsymbol{\kappa} = 0$, and simulating a single long trajectory. This is justified based on the assumption of ergodicity.[10]

5 The Gaussian Approximation

The time evolution equation for the second moments, equation (9), as mentioned earlier, is not in general a closed equation for the second moments because of the occurrence of complex higher order moments. The Gaussian approximation—which has been successfully introduced previously to treat similar closure problems that arise in the treatment of hydrodynamic interaction and internal viscosity[7, 12, 18, 20, 21]—consists essentially of reducing higher order moments to second moments, by assuming that the non-equilibrium configurational distribution function is Gaussian,

$$\psi\left(\boldsymbol{Q}_1, \ldots, \boldsymbol{Q}_{N-1}, t\right) = \mathcal{N}(t)\, \exp\left[-\frac{1}{2} \sum_{j,\,k} \boldsymbol{Q}_j \cdot (\boldsymbol{\sigma}^{-1})_{jk} \cdot \boldsymbol{Q}_k \right] \tag{36}$$

where, the $(N-1) \times (N-1)$ matrix of tensor components $\boldsymbol{\sigma}_{jk}$ (with $\boldsymbol{\sigma}_{jk} = \langle \boldsymbol{Q}_j \boldsymbol{Q}_k \rangle$ and $\boldsymbol{\sigma}_{jk} = \boldsymbol{\sigma}_{kj}^{T}$), uniquely characterizes the Gaussian distribution, and $\mathcal{N}(t)$ is the normalization factor.

For the narrow Gaussian potential, the higher order moments $\langle \boldsymbol{Q}_j \boldsymbol{F}_\mu^{(E)} \rangle$ and $\langle \boldsymbol{F}_\mu^{(E)} \boldsymbol{Q}_k \rangle$, which appear in the quantity $\boldsymbol{Y}_{jk}$ on the right hand side of equation (9), can be shown to involve averages of quantities like $\langle \boldsymbol{Q}_m \boldsymbol{Q}_n E\left(\boldsymbol{r}_\nu - \boldsymbol{r}_\mu\right) \rangle$. Using general decomposition rules for the moments of a Gaussian distribution,[7] one can show that,

$$\begin{aligned} \langle \boldsymbol{Q}_m \boldsymbol{Q}_n E\left(\boldsymbol{r}_\nu - \boldsymbol{r}_\mu\right) \rangle = {} & \frac{v\, k_{\mathrm{B}}T}{(2\pi)^{3/2}} \frac{1}{\sqrt{\det\left([\tilde{d}^2\, \mathbf{1} + \langle \boldsymbol{r}_{\nu\mu} \boldsymbol{r}_{\nu\mu} \rangle] \right)}} \times \\ & \left\{ \langle \boldsymbol{Q}_m \boldsymbol{Q}_n \rangle - \langle \boldsymbol{Q}_m \boldsymbol{r}_{\nu\mu} \rangle \cdot \left[\tilde{d}^2\, \mathbf{1} + \langle \boldsymbol{r}_{\nu\mu} \boldsymbol{r}_{\nu\mu} \rangle \right]^{-1} \cdot \langle \boldsymbol{r}_{\nu\mu} \boldsymbol{Q}_n \rangle \right\} \end{aligned} \tag{37}$$

The vector $\boldsymbol{r}_{\nu\mu}$ itself obeys a Gaussian distribution since it is a sum of Gaussian distributed bead connector vectors. As a result, the right hand side of equation (37) involves only second moments, and averages which can be evaluated by Gaussian integrals.

In the Gaussian approximation therefore, the second moment equation, equation (9), can be rewritten as,

$$\frac{d}{dt}\,\boldsymbol{\sigma}_{jk} = \boldsymbol{\kappa}\cdot\boldsymbol{\sigma}_{jk} + \boldsymbol{\sigma}_{jk}\cdot\boldsymbol{\kappa}^{T} + \frac{2k_{\mathrm{B}}T}{\zeta}\,A_{jk}\,\mathbf{1} - \frac{H}{\zeta}\sum_{m=1}^{N-1}\left[\boldsymbol{\sigma}_{jm}\,A_{mk} + A_{jm}\,\boldsymbol{\sigma}_{mk}\right] + \boldsymbol{Y}_{jk} \quad (38)$$

where,

$$\boldsymbol{Y}_{jk} = \tilde{z}\,\left(\frac{H}{\zeta}\right)\sum_{m=1}^{N-1}\left[\boldsymbol{\sigma}_{jm}\cdot\boldsymbol{\Delta}_{km} + \boldsymbol{\Delta}_{jm}\cdot\boldsymbol{\sigma}_{mk}\right] \quad (39)$$

In equation (39), $\tilde{z} = v\,(\,H/2\pi k_B T\,)^{3/2}$ is a non-dimensional parameter which measures the strength of the excluded volume interaction, and the $(N-1)\times(N-1)$ matrix of tensor components $\boldsymbol{\Delta}_{jm}$ is defined by,

$$\boldsymbol{\Delta}_{jm} = \sum_{\mu=1}^{N}\Big\{\,(B_{j+1,\,m} - B_{\mu m})\,\boldsymbol{\Pi}(\hat{\boldsymbol{\sigma}}_{j+1,\,\mu}) - (B_{jm} - B_{\mu m})\,\boldsymbol{\Pi}(\hat{\boldsymbol{\sigma}}_{j\mu})\Big\} \quad (40)$$

where, the function $\boldsymbol{\Pi}(\hat{\boldsymbol{\sigma}}_{\nu\mu})$ is given by,

$$\boldsymbol{\Pi}(\hat{\boldsymbol{\sigma}}_{\nu\mu}) = \frac{\left[d^{*2}\,\mathbf{1} + \hat{\boldsymbol{\sigma}}_{\nu\mu}\right]^{-1}}{\sqrt{\det\left(\left[d^{*2}\,\mathbf{1} + \hat{\boldsymbol{\sigma}}_{\nu\mu}\right]\right)}} \quad (41)$$

with the tensors $\hat{\boldsymbol{\sigma}}_{\nu\mu}$ defined by,

$$\hat{\boldsymbol{\sigma}}_{\nu\mu} = \hat{\boldsymbol{\sigma}}_{\nu\mu}^{T} = \hat{\boldsymbol{\sigma}}_{\mu\nu} = \frac{H}{k_B T}\sum_{j,k\,=\,\min(\mu,\nu)}^{\max(\mu,\nu)-1}\boldsymbol{\sigma}_{jk} \quad (42)$$

The parameter $d^{*} = \tilde{d}\,\sqrt{H/k_B T}$ is a non-dimensional measure of the extent of excluded volume interaction. Equation (38) is a system of $9\,(N-1)^2$ coupled ordinary differential equations for the components of the covariance matrix $\boldsymbol{\sigma}_{jk}$. As can be seen below, its solution is necessary in order to evaluate the stress tensor.

In the presence of excluded volume interactions, the Kramers expression for the stress tensor, equation (11), also involves higher order moments due to the occurrence of the term $\boldsymbol{Z}$,

$$\boldsymbol{\tau}^{p} = -n_{\mathrm{p}}H\sum_{k=1}^{N-1}\boldsymbol{\sigma}_{kk} + \boldsymbol{Z} + (N-1)\,n_{\mathrm{p}}k_{\mathrm{B}}T\,\mathbf{1} \quad (43)$$

which, in the Gaussian approximation, can be simplified (by making use of the decomposition result, equation (37)), to,

$$\boldsymbol{Z} = \frac{1}{2}\,\tilde{z}\,n_{\mathrm{p}}k_{\mathrm{B}}T\sum_{\substack{\nu,\,\mu=1\\ \nu\neq\mu}}^{N}\hat{\boldsymbol{\sigma}}_{\nu\mu}\cdot\boldsymbol{\Pi}(\hat{\boldsymbol{\sigma}}_{\nu\mu}) \quad (44)$$

In the limit of $\tilde{d}\to 0$, it is straight forward to see that the tensor $\boldsymbol{Z}$ becomes isotropic. As a result, the direct contribution to the stress tensor due to the presence of δ-function excluded volume interactions, has no influence on the rheological properties of the polymer solution.

5.1 Codeformational Memory-Integral Expansion

Linear viscoelastic properties predicted by the Gaussian approximation can be obtained by constructing a codeformational memory-integral expansion. This is done by expanding the tensors $\boldsymbol{\sigma}_{jk}$, in terms of deviations from their isotropic equilibrium solution, up to first order in velocity gradient,

$$\boldsymbol{\sigma}_{jk} = f_{jk}\,\mathbf{1} + \boldsymbol{\epsilon}_{jk} + \ldots \tag{45}$$

where, the $f_{jk}\,\mathbf{1}$ represent the equilibrium second moments in the Gaussian approximation, and $\boldsymbol{\epsilon}_{jk}$ are the first order corrections. Substituting equation (45) into equation (38), and separating the resultant equation into equations for each order in the velocity gradient, the following two equations are obtained,

Equilibrium:

$$\frac{d}{dt}\,f_{jk} = \frac{2k_{\mathrm{B}}T}{\zeta}\,A_{jk} - \left(\frac{H}{\zeta}\right)\sum_{m=1}^{N-1}\Big[f_{jm}\,(A_{mk} - \tilde{z}\,\Delta^{(0)}_{km}) + (A_{jm} - \tilde{z}\,\Delta^{(0)}_{jm})\,f_{mk}\Big] \tag{46}$$

where,

$$\Delta^{(0)}_{jm} = \sum_{\mu=1}^{N}\left[\frac{(B_{j+1,\,m} - B_{\mu m})}{\left(d^{*2} + \hat{f}_{j+1,\,\mu}\right)^{5/2}} - \frac{(B_{jm} - B_{\mu m})}{\left(d^{*2} + \hat{f}_{j\mu}\right)^{5/2}}\right] \tag{47}$$

with the quantities $\hat{f}_{\nu\mu}$ given by,

$$\hat{f}_{\nu\mu} = \left(\frac{H}{k_B T}\right)\sum_{j,k\,=\,\min(\mu,\nu)}^{\max(\mu,\nu)-1} f_{jk} \tag{48}$$

First Order:

$$\frac{d}{dt}\,\boldsymbol{\epsilon}_{jk} = (\boldsymbol{\kappa} + \boldsymbol{\kappa}^{T})\,f_{jk} - \left(\frac{H}{\zeta}\right)\sum_{m,n=1}^{N-1}\overline{A}_{jk,\,mn}\,\boldsymbol{\epsilon}_{mn} \tag{49}$$

where,

$$\begin{aligned}\overline{A}_{jk,\,mn} = {} & (A_{jm}\,\delta_{kn} + \delta_{jm}\,A_{kn}) - \tilde{z}\,(\Delta^{(0)}_{jm}\,\delta_{kn} + \delta_{jm}\,\Delta^{(0)}_{kn}) \\ & + \tilde{z}\,\left(\frac{H}{k_B T}\right)\sum_{p=1}^{N-1}\Big[f_{jp}\,\Delta^{(1)}_{kp,\,mn} + \Delta^{(1)}_{jp,\,mn}\,f_{pk}\Big]\end{aligned} \tag{50}$$

with the quantities $\Delta^{(1)}_{jp,\,mn}$ given by,

$$\Delta^{(1)}_{jp,\,mn} = \sum_{\mu=1}^{N}\left[\frac{(B_{j+1,\,p} - B_{\mu p})\,\theta(\mu,m,n,j+1)}{\left(d^{*2} + \hat{f}_{j+1,\,\mu}\right)^{7/2}} - \frac{(B_{jp} - B_{\mu p})\,\theta(\mu,m,n,j)}{\left(d^{*2} + \hat{f}_{j\mu}\right)^{7/2}}\right] \tag{51}$$

The function $\theta(\mu, m, n, \nu)$ has been introduced previously in the treatment of hydrodynamic interaction.[7] It is unity if m and n lie between μ and ν, and zero otherwise,

$$\theta(\mu, m, n, \nu) = \begin{cases} 1 & \text{if } \mu \le m, n < \nu \quad \text{or} \quad \nu \le m, n < \mu \\ 0 & \text{otherwise} \end{cases} \tag{52}$$

Introducing new indices for the pairs (j, k) and (m, n), the quantity $\overline{A}_{jk,\,mn}$ may be considered an $(N-1)^2 \times (N-1)^2$ matrix. The inverse can then be defined in the following manner,

$$\sum_{r,s=1}^{N-1} \overline{A}^{-1}_{jk,\,rs}\, \overline{A}_{rs,\,mn} = \mathbb{I}_{jk,\,mn} \tag{53}$$

where, $\mathbb{I}$ is the $(N-1)^2 \times (N-1)^2$ unit matrix $\mathbb{I}_{jk,\,mn} = \delta_{jm}\, \delta_{kn}$.

In the equilibrium second moment equation, equation (46), the term (df_{jk}/dt) on the left hand side, is identically zero. It is retained here, however, to indicate that the equation is solved for f_{jk} by numerical integration of the ODE's until steady state is reached.

Upon integrating equation (49) with respect to time, and substituting the solution into equation (43), we obtain the following expression for the first order codeformational memory-integral expansion:

$$\boldsymbol{\tau}^p = -\int_{-\infty}^{t} ds\, G(t-s)\, \boldsymbol{\gamma}_{[1]}(t, s) \tag{54}$$

where, $\boldsymbol{\gamma}_{[1]}$ is the codeformational rate-of-strain tensor,[1] and the memory function $G(t)$ is given by,

$$G(t) = \sum_{j,k=1}^{N-1} \sum_{m,n=1}^{N-1} f_{jm}\, \mathcal{H}_{jk}\, \mathcal{E}\Big[-\frac{t}{\lambda_H}\, \tilde{A} \Big]_{mk,\,nn} \tag{55}$$

In equation (55), $\lambda_H = (\zeta/4H)$ is the familiar time constant, $\mathcal{H}_{jk}$ is defined by,

$$\mathcal{H}_{jk} = n_{\mathrm{p}} H \left[\delta_{jk} - \frac{1}{2}\, \tilde{z} \sum_{\substack{\mu,\nu=1 \\ \mu \neq \nu}}^{N} \frac{d^{*2}}{\left(d^{*2} + \hat{f}_{\nu\mu} \right)^{7/2}}\, \theta(\nu, j, k, \mu) \right] \tag{56}$$

and the quantity $\tilde{A}_{jk,\,mn}$ is given by,

$$\tilde{A}_{jk,\,mn} = \sum_{r,s=1}^{N-1} \frac{1}{4}\, f^{-1}_{jr}\, \overline{A}_{rk,\,sn}\, f_{sm} \tag{57}$$

The exponential operator $\mathcal{E}\,[\,M\,]$ maps one matrix into another according to:

$$\mathcal{E}\,[\,M\,]_{\,jk,\,mn} = \mathbb{I}_{jk,\,mn} + M_{jk,\,mn} + \frac{1}{2!} \sum_{r,s=1}^{N-1} M_{jk,\,rs}\, M_{rs,\,mn} + \ldots$$

and has the useful properties,

$$\frac{d}{dt}\,\mathcal{E}\,[\,Mt\,]_{jk,mn} = \sum_{r,s=1}^{N-1} M_{jk,rs}\,\mathcal{E}\,[\,Mt\,]_{rs,mn} = \sum_{r,s=1}^{N-1} \mathcal{E}\,[\,Mt\,]_{jk,rs}\,M_{rs,mn}$$

$$\sum_{r,s=1}^{N-1} \mathcal{E}\,[\,a\,M\,]_{jk,rs}\;\mathcal{E}\,[\,b\,\mathbb{1}\,]_{rs,mn} = \mathcal{E}\,[\,a\,M + b\,\mathbb{1}\,]_{jk,mn}$$

for arbitrary constants a and b.

The codeformational memory-integral expansion, equation (54), can now be used to obtain exact expressions for material functions in small amplitude oscillatory shear flow, and for the zero shear rate viscosity and first normal stress difference coefficient in steady shear flow.

5.2 Linear Viscoelastic Properties

5.2.1 Small Amplitude Oscillatory Shear Flow

Small amplitude oscillatory shear flow is a transient experiment that is used often to characterise polymer solutions. The tensor $\boldsymbol{\kappa}(t)$ in this case is given by,

$$\boldsymbol{\kappa}(t) = \dot{\gamma}_0\,\cos\,\omega t \begin{pmatrix} 0 & 1 & 0 \\ 0 & 0 & 0 \\ 0 & 0 & 0 \end{pmatrix} \tag{58}$$

where, $\dot{\gamma}_0$ is the amplitude, and ω is the frequency of oscillations in the plane of flow. The yx component of the polymer contribution to the shear stress is then defined by,[1]

$$\tau^p_{yx} = -\eta'(\omega)\,\dot{\gamma}_0\,\cos\,\omega t - \eta''(\omega)\,\dot{\gamma}_0\,\sin\,\omega t \tag{59}$$

where η' and η'' are the material functions characterising oscillatory shear flow. They can be represented in a combined form as the complex viscosity, $\eta^* = \eta' - i\,\eta''$.

Expressions for the real and imaginary parts of the complex viscosity can be found, in terms of the relaxation modulus, from the expression $\eta^* = \int_0^\infty G(s)\,e^{-i\omega s}\,ds$. Substituting equation (55) for the memory function $G(s)$ leads to,

$$\begin{aligned} \eta'(\omega) &= \lambda_H \sum_{j,k=1}^{N-1} \sum_{m,n=1}^{N-1} \sum_{r,s=1}^{N-1} f_{jk}\,\mathcal{H}_{jm}\,\Phi^{-1}_{km,rs}\,\widetilde{A}_{rs,nn} \\ \eta''(\omega) &= \lambda_H^2\,\omega \sum_{j,k=1}^{N-1} \sum_{m,n=1}^{N-1} f_{jk}\,\mathcal{H}_{jm}\,\Phi^{-1}_{km,nn} \end{aligned} \tag{60}$$

where,

$$\Phi_{jk,mn} = \sum_{r,s=1}^{N-1} \left[\widetilde{A}_{jk,rs}\,\widetilde{A}_{rs,mn} + \lambda_H^2\,\omega^2\,\mathbb{1}_{jk,mn}\right] \tag{61}$$

5.2.2 Zero Shear Rate Limit of Steady Shear Flow

The zero shear rate viscosity $\eta_{p,0}$ and the zero shear rate first normal stress difference coefficient $\Psi_{1,0}$, can be obtained from the complex viscosity in the limit of vanishing frequency,

$$\eta_{p,0} = \lim_{\omega \to 0} \eta'(\omega)\,; \qquad \Psi_{1,0} = \lim_{\omega \to 0} \frac{2\,\eta''(\omega)}{\omega} \tag{62}$$

As a result,

$$\eta_{p,0} = 4\,\lambda_H \sum_{j,k=1}^{N-1} \sum_{m,n=1}^{N-1} \mathcal{H}_{jk}\, \overline{A}^{-1}_{jk,\,mn}\, f_{mn} \tag{63}$$

$$\Psi_{1,0} = 32\,\lambda_H^2 \sum_{j,k=1}^{N-1} \sum_{m,n=1}^{N-1} \sum_{r,s=1}^{N-1} \mathcal{H}_{jk}\, \overline{A}^{-1}_{jk,\,mn}\, \overline{A}^{-1}_{mn,\,rs}\, f_{rs} \tag{64}$$

The predictions of the zero shear rate viscometric functions by the Gaussian approximation, equations (63) and (64), are compared with the exact results, equations (24) and (25), evaluated by Brownian dynamics simulations, in section 7 below.

6 First Order Perturbation Expansion in Arbitrary Space Dimensions

The retarded motion expansion, equation (20), was obtained by carrying out a perturbation expansion of the distribution function ψ, in terms of velocity gradients. It is valid for arbitrary strength of the excluded volume interaction. In this section, by closely following the arguments in the papers by Öttinger and co-workers,[8,9,23] we derive a perturbation expansion of $\boldsymbol{\tau}^p$ in the strength of excluded volume interaction, which is valid for arbitrary shear rates. The expansion will be carried out in a space of arbitrary dimensions D, for two reasons. Firstly, as is already well known,[3,8,17] the nature of the dependence of the perturbation expansion on chain length N becomes transparent. Secondly, it can serve as a starting point for a renormalisation group analysis. While we do not carry out a complete renormalisation group calculation of the viscometric functions here, we briefly consider the renormalisation of the end-to-end vector at equilibrium, in order to examine the role of the parameter $\tilde{d}$ in the present model. An additional benefit of the perturbation expansion is a better understanding of the nature of the Gaussian approximation.

The forms of the diffusion equation and the second moment equation, equations (7) and (9) respectively, remain unchanged on going from 3 to D dimensions. The distribution function ψ can be written as $\psi_R + \psi_z$, where ψ_R is the distribution function in the absence of excluded volume, i.e. in the Rouse model, and ψ_z is the correction to first order in the strength of the excluded volume interaction. Since ψ_R is Gaussian, it has the form given by equation (36), with $\mathcal{N}(t)$ replaced by $\mathcal{N}_R(t)$, and $\boldsymbol{\sigma}_{jk}$ replaced by $\boldsymbol{\sigma}^R_{jk} = \langle \boldsymbol{Q}_j \boldsymbol{Q}_k \rangle_R$. The second moments $\langle \boldsymbol{Q}_j \boldsymbol{Q}_k \rangle$ can then be expanded to first order as, $\langle \boldsymbol{Q}_j \boldsymbol{Q}_k \rangle = \boldsymbol{\sigma}^R_{jk} + \langle \boldsymbol{Q}_j \boldsymbol{Q}_k \rangle_z$.

On substituting this expansion into equation (9), and equating terms of like order, the second moment equation can be separated into two equations, a zeroth-order equation and a first-order equation. The zeroth-order equation, which is the second moment equation of the Rouse model, is linear in $\boldsymbol{\sigma}^R_{jk}$, and has the following explicit solution,

$$\boldsymbol{\sigma}^R_{jk} = \frac{k_{\mathrm{B}}T}{H}\left\{\delta_{jk}\,\mathbf{1} + \int_{-\infty}^{t} ds\; \mathcal{E}\left[-\frac{2H}{\zeta}(t-s)A\right]_{jk} \boldsymbol{\gamma}_{[1]}(t,s)\right\} \tag{65}$$

where, the exponential operator $\mathcal{E}$, in contrast to the one in equation (55), operates on $(N-1)\times(N-1)$ matrices.

The first-order second moment equation has the form,

$$\begin{aligned}\frac{d}{dt}\left\langle \boldsymbol{Q}_j\boldsymbol{Q}_k\right\rangle_z &= \boldsymbol{\kappa}\cdot\left\langle \boldsymbol{Q}_j\boldsymbol{Q}_k\right\rangle_z + \left\langle \boldsymbol{Q}_j\boldsymbol{Q}_k\right\rangle_z\cdot\boldsymbol{\kappa}^T \\ &- \left(\frac{H}{\zeta}\right)\sum_{m=1}^{N-1}\left\{\left\langle \boldsymbol{Q}_j\boldsymbol{Q}_m\right\rangle_z A_{mk} + A_{jm}\left\langle \boldsymbol{Q}_m\boldsymbol{Q}_k\right\rangle_z\right\} + \boldsymbol{Y}^R_{jk}\end{aligned} \tag{66}$$

where, $\boldsymbol{Y}^R_{jk}$ is given by equation (10), with the averages on the right hand side evaluated with ψ_R, i.e., $\langle\cdots\rangle$ are replaced with $\langle\cdots\rangle_R$. Since ψ_R is a Gaussian distribution, the decomposition result, equation (37), with $(2\pi)^{3/2}$ replaced by $(2\pi)^{D/2}$ and $\langle\cdots\rangle$ are replaced with $\langle\cdots\rangle_R$, can be used to reduce $\boldsymbol{Y}^R_{jk}$ to a function of second moments alone. This leads to,

$$\boldsymbol{Y}^R_{jk} = \tilde{z}_D\left(\frac{H}{\zeta}\right)\sum_{m=1}^{N-1}\left[\boldsymbol{\sigma}^R_{jm}\cdot\boldsymbol{\Delta}^R_{km} + \boldsymbol{\Delta}^R_{jm}\cdot\boldsymbol{\sigma}^R_{mk}\right] \tag{67}$$

In equation (67), $\tilde{z}_D = v\,(\,H/2\pi k_BT\,)^{D/2}$ is an extension of the earlier definition of $\tilde{z}$ to D dimensions, and $\boldsymbol{\Delta}^R_{jm}$ is given by equation (40), with $\boldsymbol{\sigma}_{jk}$ replaced by $\boldsymbol{\sigma}^R_{jk}$ in the definition of $\hat{\boldsymbol{\sigma}}_{\mu\nu}$ on the right hand side. Equation (66) is a system of linear inhomogeneous ordinary differential equations, whose solution is,

$$\begin{aligned}\left\langle \boldsymbol{Q}_j\boldsymbol{Q}_k\right\rangle_z &= \sum_{r,s=1}^{N-1}\int_{-\infty}^{t} ds\,\mathcal{E}\left[-\frac{H}{\zeta}(t-s)A\right]_{jr}\boldsymbol{E}(t,s)\cdot\boldsymbol{Y}^R_{rs}(s)\cdot\boldsymbol{E}^T(t,s) \\ &\times\ \mathcal{E}\left[-\frac{H}{\zeta}(t-s)A\right]_{sk}\end{aligned} \tag{68}$$

where, $\boldsymbol{E}$ is the displacement gradient tensor.[1]

It is immediately clear from equation (66) that the Gaussian approximation is exact to first order in the strength of excluded volume interaction. This follows from the fact that it could have also been derived by expanding equation (38) (generalised to D dimensions, i.e., with $\tilde{z}$ replaced by $\tilde{z}_D$), to first order in $\tilde{z}_D$. It will be seen later that this property of the Gaussian approximation, is helpful in elucidating its nature.

The first order perturbation expansion for the stress tensor can be obtained by expanding Kramers expression, equation (11), to first order in z. After reducing complex moments evaluated with the Rouse distribution function to second moments, the stress tensor can be shown to depend only on second moments through the relation,

$$\boldsymbol{\tau}^p = -n_{\rm p} H \sum_{k=1}^{N-1} \boldsymbol{\sigma}^R_{kk} - n_{\rm p} H \sum_{k=1}^{N-1} \langle \boldsymbol{Q}_k \boldsymbol{Q}_k \rangle_z + \boldsymbol{Z}^R + (N-1)\, n_{\rm p} k_{\rm B} T\, \mathbf{1} \qquad (69)$$

where, $\boldsymbol{Z}^R$ is given by equation (44), with $\tilde{z}$ replaced by $\tilde{z}_D$, and $\boldsymbol{\sigma}_{jk}$ replaced by $\boldsymbol{\sigma}^R_{jk}$ in the definition of $\hat{\boldsymbol{\sigma}}_{\mu\nu}$, on the right hand side. Equations (65) and (68) may then be used to derive the following first order perturbation expansion for the stress tensor in arbitrary homogeneous flows and arbitrary space dimensions,

$$\begin{aligned} \boldsymbol{\tau}^p &= -n_{\rm p} k_B T \sum_{r,s=1}^{N-1} \int_{-\infty}^{t} ds\, \mathcal{E}\left[-\frac{2H}{\zeta}(t-s)A\right]_{sr} \boldsymbol{E}(t,s) \cdot \left\{ \left(\boldsymbol{\kappa}(s) + \boldsymbol{\kappa}^T(s)\right)\, \delta_{rs} \right. \\ &+ \left. \left(\frac{H}{k_{\rm B}T}\right)\, \boldsymbol{Y}^R_{rs}(s) \right\} \cdot \boldsymbol{E}^T(t,s) + \boldsymbol{Z}^R + (N-1)\, n_{\rm p} k_{\rm B} T\, \mathbf{1} \end{aligned} \qquad (70)$$

Note that $\boldsymbol{Z}^R$, the direct contribution to the stress tensor, is isotropic only in the limit $\tilde{d} \to 0$. We now consider the special case of steady shear flow, and obtain the zero shear rate viscometric functions by going to the limit $\lambda_H \dot{\gamma} \to 0$, in the expressions for the viscometric functions.

6.1 Steady Shear Flow

In a D-dimensional coordinate system, the tensor $\boldsymbol{\kappa}$ has the following matrix representation,

$$\boldsymbol{\kappa} = \dot{\gamma} \begin{pmatrix} 0 & 1 & 0 & . & . & . \\ 0 & 0 & 0 & . & . & . \\ 0 & 0 & 0 & . & . & . \\ . & . & . & . & & \\ . & . & . & & . & \\ . & . & . & & & . \end{pmatrix} \qquad (71)$$

The forms of the tensors $\boldsymbol{\gamma}_{[1]}$ and $\boldsymbol{E}$, in steady shear flow, have been tabulated in reference 1. On generalising these expressions to D dimensions, the time integrations in equations (65), (68), and (70) can be carried out. The resultant expressions are discussed in turn below.

In steady shear flow, the second moment $\boldsymbol{\sigma}^R_{jk}$ is given by,

$$\boldsymbol{\sigma}^R_{jk} = \frac{k_{\rm B}T}{H} \left\{ \delta_{jk}\, \mathbf{1} + 2\lambda_H C_{jk} \left(\boldsymbol{\kappa} + \boldsymbol{\kappa}^T\right) + 8\lambda_H^2 C^2_{jk} \left(\boldsymbol{\kappa} \cdot \boldsymbol{\kappa}^T\right) \right\} \qquad (72)$$

This expression is required to explicitly evaluate all the averages carried out in this section with the Rouse distribution function ψ_R.

The first order correction to the second moments has the following form in steady shear flow,

$$\begin{aligned}\langle \boldsymbol{Q}_j \boldsymbol{Q}_k \rangle_z &= \left(\frac{\zeta}{H}\right) \sum_{r,s=1}^{N-1} R^{-1}_{jk,\,rs}\, \boldsymbol{Y}^R_{rs} \\ &+ \left(\frac{\zeta}{H}\right)^2 \sum_{r,s=1}^{N-1} \sum_{m,n=1}^{N-1} R^{-1}_{jk,\,mn}\, R^{-1}_{mn,\,rs} \left[\boldsymbol{\kappa}\cdot \boldsymbol{Y}^R_{rs} + \boldsymbol{Y}^R_{rs}\cdot \boldsymbol{\kappa}^T\right] \\ &+ 2\left(\frac{\zeta}{H}\right)^3 \sum_{r,s=1}^{N-1} \sum_{m,n=1}^{N-1} \sum_{l,p=1}^{N-1} R^{-1}_{jk,\,mn}\, R^{-1}_{mn,\,lp}\, R^{-1}_{lp,\,rs} \left[\boldsymbol{\kappa}\cdot \boldsymbol{Y}^R_{rs}\cdot \boldsymbol{\kappa}^T\right] \end{aligned} \quad (73)$$

where, the $(N-1)^2 \times (N-1)^2$ matrix $R_{jk,\,mn}$ is defined by, $R_{jk,\,mn} = A_{jm}\,\delta_{kn} + \delta_{jm}\,A_{kn}$. This expression, though valid even away from equilibrium, will be used here subsequently only to find the end-to-end vector at equilibrium.

The stress tensor in steady shear flow has the form,

$$\begin{aligned}\boldsymbol{\tau}^p &= -n_{\rm p} k_B T \sum_{j=1}^{N-1} \left[2\lambda_H\, C_{jj}\left(\boldsymbol{\kappa} + \boldsymbol{\kappa}^T\right) + 8\lambda_H^2\, C^2_{jj}\left(\boldsymbol{\kappa}\cdot\boldsymbol{\kappa}^T\right)\right] \\ &- n_{\rm p} H \sum_{j,k=1}^{N-1} \Big\{2\lambda_H\, C_{kj}\, \boldsymbol{Y}^R_{jk} + 4\lambda_H^2\, C^2_{kj}\left[\boldsymbol{\kappa}\cdot\boldsymbol{Y}^R_{jk} + \boldsymbol{Y}^R_{jk}\cdot\boldsymbol{\kappa}^T\right] \\ &+ 16\lambda_H^3\, C^3_{kj}\left[\boldsymbol{\kappa}\cdot\boldsymbol{Y}^R_{jk}\cdot\boldsymbol{\kappa}^T\right]\Big\} + \boldsymbol{Z}^R \end{aligned} \quad (74)$$

A similar expression, without the $\boldsymbol{Z}^R$ term, has been derived by Öttinger[9] in his renormalisation group treatment of excluded volume effects—within the framework of polymer kinetic theory—using a δ-function excluded volume potential.

The next step is to explicitly evaluate the tensors $\boldsymbol{Y}^R_{jk}$ and $\boldsymbol{Z}^R$, in terms of the velocity gradient $\boldsymbol{\kappa}$ and the Kramers matrix C_{kj}, by using equation (72) for $\boldsymbol{\sigma}^R_{jk}$. The resultant expressions are then substituted into equation (74), and after a very lengthy calculation, the following explicit expression for the *excluded volume contribution* to the stress tensor, correct to first order in $\tilde{z}_D$, is obtained,

$$\begin{aligned}\boldsymbol{\tau}^p_{(E)} &= -\frac{1}{8\lambda_H}\, n_{\rm p} k_B T\, \tilde{z}_D \sum_{\substack{\mu,\nu=1\\ \mu\neq\nu}}^{N} \frac{1}{\left(d^{*2} + S^{(0)}_{\mu\nu}\right)^{1+D/2}\, e_{\mu\nu}(\dot\gamma)^{3/2}} \Big\{\left(\alpha^{(0)}_{\mu\nu} - \beta^{(0)}_{\mu\nu}\right)\mathbf{1} \\ &+ \left(\alpha^{(1)}_{\mu\nu} - \beta^{(1)}_{\mu\nu}\right)\left(\boldsymbol{\kappa} + \boldsymbol{\kappa}^T\right) + \left(\alpha^{(2)}_{\mu\nu} - \beta^{(2)}_{\mu\nu}\right)\left(\boldsymbol{\kappa}\cdot\boldsymbol{\kappa}^T\right) + \left(\alpha^{(3)}_{\mu\nu} - \beta^{(3)}_{\mu\nu}\right)\left(\boldsymbol{\kappa}^T\cdot\boldsymbol{\kappa}\right) \\ &+ \left(\alpha^{(4)}_{\mu\nu} - \beta^{(4)}_{\mu\nu}\right)\left(\boldsymbol{\kappa}\cdot\boldsymbol{\kappa}^T\cdot\boldsymbol{\kappa}\right) + \left(\alpha^{(5)}_{\mu\nu} - \beta^{(5)}_{\mu\nu}\right)\left(\boldsymbol{\kappa}^T\cdot\boldsymbol{\kappa}\cdot\boldsymbol{\kappa}^T\right) \\ &+ \left(\alpha^{(6)}_{\mu\nu} - \beta^{(6)}_{\mu\nu}\right)\left(\boldsymbol{\kappa}\cdot\boldsymbol{\kappa}^T\cdot\boldsymbol{\kappa}\cdot\boldsymbol{\kappa}^T\right)\Big\} \end{aligned} \quad (75)$$

where, the functions $\alpha^{(j)}_{\mu\nu}$ and $\beta^{(j)}_{\mu\nu}$; $(j = 0, 1, \ldots, 6)$, which represent the *indirect* and *direct* contributions respectively, are given in Tables 1 and 2, the function $e_{\mu\nu}(\dot\gamma)$ is

Table 1: Functions, appearing in equation (75), representing the *indirect* excluded volume contributions to the stress tensor in steady shear flow. The quantity Ω is defined by, $\Omega = 4/(d^{*2} + S_{\mu\nu}^{(0)})^2$.

$$\alpha_{\mu\nu}^{(0)} = \lambda_H\, S_{\mu\nu}^{(0)}\, \Omega \left[\left(d^{*2} + S_{\mu\nu}^{(0)} \right)^2 + \lambda_H^2 \dot{\gamma}^2 \left\{ 2\, S_{\mu\nu}^{(2)} \left(d^{*2} + S_{\mu\nu}^{(0)} \right) - S_{\mu\nu}^{(1)}\, S_{\mu\nu}^{(1)} \right\} \right]$$

$$\alpha_{\mu\nu}^{(1)} = \lambda_H^2\, S_{\mu\nu}^{(1)}\, \Omega \left[\left(d^{*2} + S_{\mu\nu}^{(0)} \right) \left(2d^{*2} + S_{\mu\nu}^{(0)} \right) + 2\lambda_H^2 \dot{\gamma}^2 \left\{ 2\, S_{\mu\nu}^{(2)} \left(d^{*2} + S_{\mu\nu}^{(0)} \right) - S_{\mu\nu}^{(1)}\, S_{\mu\nu}^{(1)} \right\} \right]$$

$$\alpha_{\mu\nu}^{(2)} = \lambda_H^3\, \Omega \left[3\, d^{*2} + 2\, S_{\mu\nu}^{(0)} + 6\lambda_H^2 \dot{\gamma}^2\, S_{\mu\nu}^{(2)} + 2\, S_{\mu\nu}^{(2)} \left(d^{*2} + S_{\mu\nu}^{(0)} \right) - S_{\mu\nu}^{(1)}\, S_{\mu\nu}^{(1)} \right]$$

$$\alpha_{\mu\nu}^{(3)} = -\lambda_H^3\, \Omega\, S_{\mu\nu}^{(1)}\, S_{\mu\nu}^{(1)}\, d^{*2}$$

$$\alpha_{\mu\nu}^{(4)} = \lambda_H^4\, S_{\mu\nu}^{(1)}\, \Omega \left[2\, S_{\mu\nu}^{(1)}\, S_{\mu\nu}^{(1)} - 3\, S_{\mu\nu}^{(2)} \left(d^{*2} + S_{\mu\nu}^{(0)} \right) \right]$$

$$\alpha_{\mu\nu}^{(5)} = \alpha_{\mu\nu}^{(4)}$$

$$\alpha_{\mu\nu}^{(6)} = 2\, \lambda_H^5\, \Omega \left[3\, S_{\mu\nu}^{(2)} \left\{ S_{\mu\nu}^{(1)}\, S_{\mu\nu}^{(1)} - S_{\mu\nu}^{(2)} \left(d^{*2} + S_{\mu\nu}^{(0)} \right) \right\} - 2\, S_{\mu\nu}^{(3)}\, S_{\mu\nu}^{(1)} \left(d^{*2} + S_{\mu\nu}^{(0)} \right) \right]$$

---

defined by,

$$e_{\mu\nu}(\dot{\gamma}) = 1 + \frac{\lambda_H^2 \dot{\gamma}^2}{\left(d^{*2} + S_{\mu\nu}^{(0)} \right)^2} \left[2 \left(d^{*2} + S_{\mu\nu}^{(0)} \right) S_{\mu\nu}^{(2)} - S_{\mu\nu}^{(1)}\, S_{\mu\nu}^{(1)} \right] \tag{76}$$

and the quantities $S_{\mu\nu}^{(m)}$, which occur in these functions and which were introduced earlier by Öttinger,[9] are defined by,

$$S_{\mu\nu}^{(m)} = 2^m \sum_{j,k=1}^{N-1} \theta(\mu, j, k, \nu)\, C_{jk}^m \tag{77}$$

Equation (75) for the stress tensor can be used to find the *excluded volume contributions* to the viscometric functions, correct to first order in $\tilde{z}_D$, by using the definitions in equations (22),

$$\begin{aligned} \eta_p^{(E)} &= \frac{1}{2}\, \lambda_H^2\, \tilde{z}_D \sum_{\substack{\mu,\nu=1 \\ \mu \neq \nu}}^{N} \frac{1}{\left(d^{*2} + S_{\mu\nu}^{(0)} \right)^{2+D/2} e_{\mu\nu}(\dot{\gamma})^{3/2}} \left[S_{\mu\nu}^{(0)}\, S_{\mu\nu}^{(1)} + \lambda_H^2 \dot{\gamma}^2\, S_{\mu\nu}^{(1)} S_{\mu\nu}^{(2)} \right. \\ &+ \left. d^{*2}\, S_{\mu\nu}^{(1)} \right] \end{aligned} \tag{78}$$

Table 2: Functions, appearing in equation (75), representing the *direct* excluded volume contributions to the stress tensor in steady shear flow. The quantity Ω is defined by, $\Omega = 4/(d^{*2} + S^{(0)}_{\mu\nu})^2$.

$$\beta^{(0)}_{\mu\nu} = \lambda_H S^{(0)}_{\mu\nu}\,\Omega\left[\left(d^{*2}+S^{(0)}_{\mu\nu}\right)^2 + \lambda_H^2\dot\gamma^2\left\{2\,S^{(2)}_{\mu\nu}\left(d^{*2}+S^{(0)}_{\mu\nu}\right) - S^{(1)}_{\mu\nu}\,S^{(1)}_{\mu\nu}\right\}\right]$$

$$\beta^{(1)}_{\mu\nu} = \lambda_H^2 S^{(1)}_{\mu\nu}\,\Omega\left[\left(d^{*2}+S^{(0)}_{\mu\nu}\right)d^{*2} + \lambda_H^2\dot\gamma^2\left\{2\,S^{(2)}_{\mu\nu}\left(d^{*2}+S^{(0)}_{\mu\nu}\right) - S^{(1)}_{\mu\nu}\,S^{(1)}_{\mu\nu}\right\}\right]$$

$$\beta^{(2)}_{\mu\nu} = \lambda_H^3\,\Omega\left[d^{*2} + 2\lambda_H^2\dot\gamma^2\,S^{(2)}_{\mu\nu} + 2\,S^{(2)}_{\mu\nu}\left(d^{*2}+S^{(0)}_{\mu\nu}\right) - S^{(1)}_{\mu\nu}\,S^{(1)}_{\mu\nu}\right]$$

$$\beta^{(3)}_{\mu\nu} = -\lambda_H^3\,\Omega\,S^{(1)}_{\mu\nu}\,S^{(1)}_{\mu\nu}\,d^{*2}$$

$$\beta^{(4)}_{\mu\nu} = \lambda_H^4 S^{(1)}_{\mu\nu}\,\Omega\left[S^{(1)}_{\mu\nu}\,S^{(1)}_{\mu\nu} - 2\,S^{(2)}_{\mu\nu}\left(d^{*2}+S^{(0)}_{\mu\nu}\right)\right]$$

$$\beta^{(5)}_{\mu\nu} = \beta^{(4)}_{\mu\nu}$$

$$\beta^{(6)}_{\mu\nu} = 2\,\lambda_H^5\,\Omega\left[S^{(1)}_{\mu\nu}\,S^{(1)}_{\mu\nu} - 2\,S^{(2)}_{\mu\nu}\left(d^{*2}+S^{(0)}_{\mu\nu}\right)\right]$$

$$\begin{aligned}\Psi_1^{(E)} &= \lambda_H^2\,\tilde z_D \sum_{\substack{\mu,\nu=1\\ \mu\neq\nu}}^{N} \frac{1}{\left(d^{*2}+S^{(0)}_{\mu\nu}\right)^{2+D/2}\,e_{\mu\nu}(\dot\gamma)^{3/2}} \\ &\times \left[2\,S^{(2)}_{\mu\nu}\left(d^{*2}+S^{(0)}_{\mu\nu}\right) - S^{(1)}_{\mu\nu}\,S^{(1)}_{\mu\nu} + \lambda_H^2\dot\gamma^2\left(3\,S^{(2)}_{\mu\nu}\,S^{(2)}_{\mu\nu} - 2\,S^{(3)}_{\mu\nu}\,S^{(1)}_{\mu\nu}\right)\right] \qquad (79)\end{aligned}$$

$$\Psi_2^{(E)} = \frac{1}{8\lambda_H}\,n_{\rm p}k_BT\,\tilde z_D \sum_{\substack{\mu,\nu=1\\ \mu\neq\nu}}^{N} \frac{\alpha^{(3)}_{\mu\nu} - \beta^{(3)}_{\mu\nu}}{\left(d^{*2}+S^{(0)}_{\mu\nu}\right)^{1+D/2}\,e_{\mu\nu}(\dot\gamma)^{3/2}} = 0 \qquad (80)$$

These expressions have been derived earlier by Öttinger[9] in the limit $\tilde d \to 0$. It is clear from equation (80) that the second normal stress difference coefficient is zero because the indirect and direct excluded volume contributions cancel each other out. When $\tilde d \to 0$, however, both the quantities $\alpha^{(3)}_{\mu\nu}$ and $\beta^{(3)}_{\mu\nu}$ are identically zero.

The first order perturbation theory predictions of the zero shear rate viscometric functions, obtained from equations (78) and (79) in the limit $\lambda_H\dot\gamma = 0$, for the special case of $D = 3$, are compared with exact Brownian dynamics simulations and the Gaussian approximation in section 7. We first, however, examine the role of the parameter $\tilde d$ in the present model, by considering the renormalisation of the end-to-end vector at equilibrium.

6.2 Renormalisation of the Equilibrium End-to-End Vector

The second moment of the end-to-end vector $\boldsymbol{r}$ at equilibrium is given by the expression,

$$\langle \boldsymbol{r}\boldsymbol{r} \rangle_{\mathrm{eq}} = \sum_{j,k=1}^{N-1} \langle \boldsymbol{Q}_j \boldsymbol{Q}_k \rangle_{\mathrm{eq}} \tag{81}$$

It is straight forward to show that at equilibrium, the quantity $\boldsymbol{Y}^R_{jk}$ has the form,

$$\boldsymbol{Y}^R_{jk}\Big|_{\mathrm{eq}} = \tilde{z}_D \, \frac{k_{\mathrm{B}}T}{2\zeta} \sum_{\substack{\mu,\nu=1 \\ \mu \neq \nu}}^{N} \frac{1}{\left(d^{*2} + S^{(0)}_{\mu\nu}\right)^{1+D/2}} \left(\sum_{m,n=1}^{N-1} \theta(\mu,m,n,\nu)\, R_{jk,mn} \right) \mathbf{1} \tag{82}$$

On combining equation (81), equations (72) and (73) (with $\boldsymbol{\kappa} = 0$), and equation (82), the following expression for the mean square end-to-end vector at equilibrium, correct to first order in $\tilde{z}_D$, is obtained,

$$\langle \boldsymbol{r}^2 \rangle_{\mathrm{eq}} = \frac{D\, k_{\mathrm{B}}T}{H} \left[(N-1) + \frac{1}{2}\, \tilde{z}_D \sum_{\substack{\mu,\nu=1 \\ \mu \neq \nu}}^{N} \frac{|\mu - \nu|^2}{\left(d^{*2} + |\mu - \nu|\right)^{1+D/2}} \right] \tag{83}$$

We now consider the limit of a large number of beads, N. In this limit, the sums in equation (83) can be replaced by integrals. Introducing the following variables,

$$x = \frac{\mu}{N}; \quad y = \frac{\nu}{N}; \quad d = \frac{d^*}{\sqrt{N}} \tag{84}$$

and exploiting the symmetry in x and y, we obtain,

$$\langle \boldsymbol{r}^2 \rangle_{\mathrm{eq}} = \frac{D\, k_{\mathrm{B}}T}{H}\, N \left\{ 1 + \tilde{z}_D\, N^{\epsilon/2} \int_0^1 dx \int_{\substack{0 \\ x > y+c}}^{x} dy \; \frac{(x-y)^2}{\left(d^2 + x - y\right)^{3-\epsilon/2}} \right\} \tag{85}$$

where, $\epsilon = 4 - D$, and c is a *cutoff* parameter, of order $1/N$, which accounts for the fact that $\mu \neq \nu$.

It is clear from equation (85) that the excluded volume corrections to the Rouse end-to-end vector are proportional to $\tilde{z}_D\, N^{\epsilon/2}$. As a result, the proper perturbation parameter to choose is $z_D = \tilde{z}_D\, N^{\epsilon/2}$, and not $\tilde{z}_D$. This is a very well known result of the theory of polymer solutions,[3,4,17] and indicates that for $D = 3$, a perturbation expansion in $\tilde{z}_D$ becomes useless for long chains. Useful results can be extracted only when D is close to 4 dimensions.

The integrals in equation (85) can be performed analytically. Since the resultant expression is lengthy and not very instructive, it is not reproduced here. However, the form of equation (85) leads to a very valuable insight. Defining the quantity α, which is frequently used to represent the *swelling* of the polymer chain at equilibrium due to excluded volume effects,

$$\alpha^2 = \frac{\langle \boldsymbol{r}^2 \rangle_{\mathrm{eq}}}{\langle \boldsymbol{r}^2 \rangle^R_{\mathrm{eq}}} \tag{86}$$

we can see that in the limit of long chains, $\alpha = \alpha\,(z_D, d\,)$. In other words, α depends asymptotically only on the parameters z_D and d, and not on the chain length N. We shall see later that this insight is very useful in understanding the results of Brownian dynamics simulations, and the Gaussian approximation.

The integrals in equation (85), as mentioned above, can be performed analytically, and the resultant expression can be expanded as a power series in ϵ. For the purposes of renormalisation, the expansion is required only up to order ϵ^0. Carrying out the expansion in ϵ, retaining terms up to this order, and neglecting the cutoff c, one obtains,

$$\langle \boldsymbol{r}^2 \rangle_{\rm eq} = \frac{D\,k_{\rm B}T}{H}\,N\left\{1 + \tilde{z}_D\,N^{\epsilon/2}\,\left[(1+3\,d^2)\{(1+d^2)^{\epsilon/2} - d^{\epsilon}\}\right]\left[\frac{2}{\epsilon} - K(d,\epsilon)\right]\right\} \tag{87}$$

where,

$$K(d,\epsilon) = \frac{\frac{3}{2}\,d^{\epsilon}\,(1+d^2) + (1-\frac{3}{2}\,d^4)\,(1+d^2\,)^{-1+\epsilon/2}}{(1+3\,d^2\,)\,[(1+d^2)^{\epsilon/2} - d^{\epsilon}]} \tag{88}$$

If we keep ϵ finite and set $d = 0$ in equation (87), we get the expression for a δ-function excluded volume potential. This expression has a $(1/\epsilon)$ singularity which arises because of the neglect of the cutoff. As has been pointed out by Öttinger,[9] a renormalisation group analysis can be performed to get rid of the $(1/\epsilon)$ singularity, or, if the cutoff is retained, renormalisation group analysis can be used to get rid of the cutoff dependence. Curiously, when $d \neq 0$, the parameter d plays a role similar to the cutoff parameter c. This follows from the fact that equation (87) is free of any singularities as $\epsilon \to 0$.

In order to perform the renormalisation of the end-to-end vector, we follow standard practice,[8,9] and introduce the concept of a polymer segment. The polymer segment is used to represent a unit of molecular weight, free of any mechanical interpretation. The polymer chain is thus assumed to consist of $N_{\rm s}$ segments, each consisting of $L_{\rm s}$ beads, so that $N = N_{\rm s}\,L_{\rm s}$. The segments are introduced in order to remove the ambiguities associated with the arbitrariness in the choice of the number of beads in a polymer chain. The size of a polymer segment, L, is assumed to be related to the number of beads in a segment $L_{\rm s}$, through the relation $L = Z_N\,L_{\rm s}$. Introducing a non-dimensional excluded volume parameter,

$$u_{\rm s} = v\left[\frac{k_{\rm B}T}{H}\right]^{-D/2}(1+3\,d^2\,)\left[(1+d^2)^{\epsilon/2} - d^{\epsilon}\right]L^{\epsilon/2} \tag{89}$$

equation (87) can be rewritten in terms of $N_{\rm s}$, $u_{\rm s}$, and L as,

$$\langle \boldsymbol{r}^2 \rangle_{\rm eq} = \frac{D\,k_{\rm B}T}{H}\,L\,N_{\rm s}\,Z_N^{-1}\left\{1 + \frac{u_{\rm s}}{4\pi^2}\,(2\pi N_{\rm s})^{\epsilon/2}\,Z_N^{-\epsilon/2}\left[\frac{2}{\epsilon} - K(d,\epsilon)\right]\right\} \tag{90}$$

The next step in the renormalisation procedure consists of introducing a segment excluded volume parameter u, which, by renormalising the *bare* excluded volume

parameter $u_{\rm s}$, takes into account all the excluded volume interactions between the many monomers within a segment,

$$u = Z_u \, u_{\rm s} \tag{91}$$

The parameters $u_{\rm s}$ and $L_{\rm s}$ are then expected to be functions of u, and expanded in a Taylor's series,

$$u_{\rm s} = u(1 + Au + \ldots) \, ; \quad L_{\rm s} = L(1 + Bu + \ldots)$$

so that, for small u,

$$\begin{aligned} Z_u &= 1 - Au + \cdots \\ Z_N &= 1 - Bu + \cdots \end{aligned} \tag{92}$$

Substituting equations (92) into equation (90), keeping only first order terms in u, and expanding $(2\pi N_{\rm s})^{\epsilon/2}$ to first order in ϵ, we have,

$$\langle \boldsymbol{r}^2 \rangle_{\rm eq} = \frac{D \, k_{\rm B} T}{H} \, L \, N_{\rm s} \left\{ 1 + \frac{u}{2\pi^2} \left[\frac{1}{\epsilon} + \frac{1}{2} \, \ln(2\pi N_{\rm s}) - \frac{K(d,\epsilon)}{2} + 2\pi^2 B \right] \right\} \tag{93}$$

Making the choice,

$$B = -\frac{1}{2\pi^2 \epsilon} + \frac{K(d,\epsilon)}{4\pi^2}$$

gets rid of all the *micro-structure* dependent terms in equation (93), and leads to,

$$\langle \boldsymbol{r}^2 \rangle_{\rm eq} = \frac{D \, k_{\rm B} T}{H} \, L \, N_{\rm s} \left\{ 1 + \frac{u}{4\pi^2} \ln(2\pi N_{\rm s}) \right\} \tag{94}$$

In the limit $d \to 0$, since $K(d,\epsilon)$ is a constant equal to one, the quantity B is usually chosen to be equal to $(-1/2\pi^2\epsilon)$. As a result, an additional term equal to $(-u/4\pi^2)$, appears within the braces on the right hand side of equation (94).

The form of equation (94) is not consistent with the expectation of a power law dependence of $\langle \boldsymbol{r}^2 \rangle_{\rm eq}$ on $N_{\rm s}$. As a result, renormalisation group analysis proceeds by exponentiating the first order perturbation expansion result,

$$\langle \boldsymbol{r}^2 \rangle_{\rm eq} = \frac{D \, k_{\rm B} T}{H} \, L \, (2\pi)^{\frac{u}{4\pi^2}} \, N_{\rm s}^{2\,\nu} \tag{95}$$

where, $\nu = \frac{1}{2} + \frac{u}{8\pi^2}$. The exponent ν is then obtained by substituting the *fixed point* value, $u = u^*$, for u.[9] The fixed point denotes the regime where the properties of the infinitely long polymer chain have a power law dependence on $N_{\rm s}$, and the fixed point value is found by setting $Z_u = 0$. For instance, in the case of a δ-function excluded volume potential, the fixed point value is known to be $u^* = (\pi^2\epsilon/2)$, which leads to an exponent, $\nu = \frac{1}{2} + \frac{1}{16}\,\epsilon$.

It is not possible to find the fixed point value u^* in the present model by only considering the renormalisation of $\langle \boldsymbol{r}^2 \rangle_{\rm eq}$, since the quantity A does not appear

in equation (93), which is correct only to first order in u. However, we do not require the fixed point value in order to make the following argument. The form of equation (95) suggests that, in the long chain limit, for chains with a very large bare excluded volume parameter u_s (which is a consequence of $Z_u = 0$, see equation (91)), the parameter d, except for possibly modifying the *prefactor*, does not in any way alter the N_s dependence of the mean square end-to-end vector. The validity of the above renormalisation procedure can only be confirmed by ensuring that the *same* definition of u_s and choice of parameter B made here, cancels the micro-structure dependence of all the other observable quantities in the theory, such as η_p, Ψ_1, etc. This has not been pursued here as it is considered outside the scope of the present work. However, it is the accepted wisdom in static theories of polymer solutions that the choice of the excluded volume potential does not influence the scaling of observables with molecular weight. Furthermore, dimensionless ratios constructed from observable quantities are also expected to be free of micro-structure dependence. In our case this implies that, for $z_D >> 1$, universal ratios can be expected to be independent of the choice of the value of d.

We shall make use of the insight gained in this section in our analysis of the results of the Gaussian approximation below. This is justified since the Gaussian approximation and renormalisation group analysis are similar in a certain sense; both are exact to first order in $\tilde{z}_D$, and both account for an infinite number of higher order contributions.

7 Equilibrium Swelling and Zero Shear Rate Viscometric Functions

The prediction of equilibrium properties and zero shear rate viscometric functions, by Brownian dynamics simulations, the Gaussian approximation, and the first order perturbation expansion in 3 dimensions, are compared in this section. Before doing so, it is appropriate to note that an equilibrium property, frequently defined in static theories of polymer solutions, namely, the swelling of the radius of gyration, α_g^2, can be found from the following expression,

$$\alpha_g^2 = \frac{\langle R_g^2 \rangle_{\rm eq}}{\langle R_g^2 \rangle_{\rm eq}^R} = \frac{\eta_{p,0}}{\eta_{p,0}^R} \tag{96}$$

because of the relation between the radius of gyration and the zero shear rate viscosity, equation (28). Plots of α_g^2 in this section must, therefore, also be seen as plots of the ratio of the zero shear rate viscosity in the presence of excluded volume interactions to the zero shear rate viscosity in the Rouse model.

Figures 1 to 3 are plots of α^2, α_g^2 and $(\Psi_{1,0}/\Psi_{1,0}^R)$ versus d^*, respectively, at a constant value of $\tilde{z} = 0.5$, for three different chain lengths, $N = 3$, $N = 6$ and $N = 12$. The squares, circles and triangles are exact results of Brownian dynamics simulations for the narrow Gaussian potential. The Brownian dynamics simulations were used to evaluate the equilibrium averages that occur in the definitions

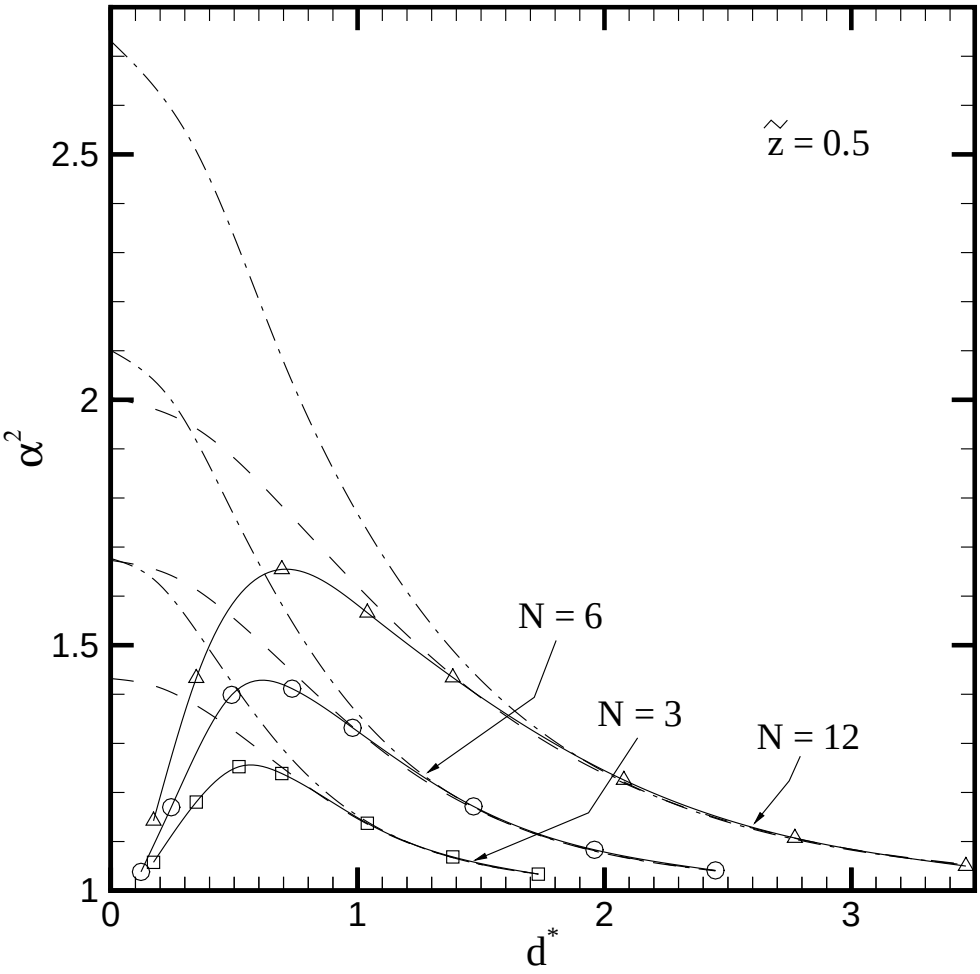

Figure 1: Equilibrium swelling of the end-to-end vector versus the extent of excluded volume interaction d^*, at a constant value of the strength of the interaction $\tilde{z}$, for three different values of chain length, N. The squares, circles and triangles are results of Brownian dynamics simulations, the dashed and dot-dashed lines are the approximate predictions of the Gaussian approximation, and the first order perturbation theory, respectively. The error bars in the Brownian dynamics simulations are smaller than the size of the symbols, and the continuous curves through the symbols are drawn for guiding the eye.

of these quantities (see equations (86), (29) and (25)). The dashed lines are the predictions of the Gaussian approximation. Note that in the Gaussian approximation, $\alpha^2 = (\hat{f}_{1N}/\hat{f}^R_{1N})$, while the zero shear rate properties $\eta_{p,0}$ and $\Psi_{1,0}$ are given by equations (63) and (64), respectively. The dot-dashed curves are the predictions of the first order perturbation theory, where, the swelling α^2 is evaluated using equation (86), with $\langle \boldsymbol{r}^2 \rangle_{\rm eq}$ given by equation (83), while $\eta_{p,0}$ and $\Psi_{1,0}$ are found from equations (78) and (79) respectively, in the limit $\lambda_H \dot{\gamma} \to 0$.

In the limit $d^* \to 0$ and for large values of d^*, for all the values of chain length N, the Brownian dynamics simulations reveal that equilibrium and zero shear rate properties tend to Rouse model values. In the case of α^2 and α^2_g, this is expected because of the rigorous result, equation (33). An immediate implication of this

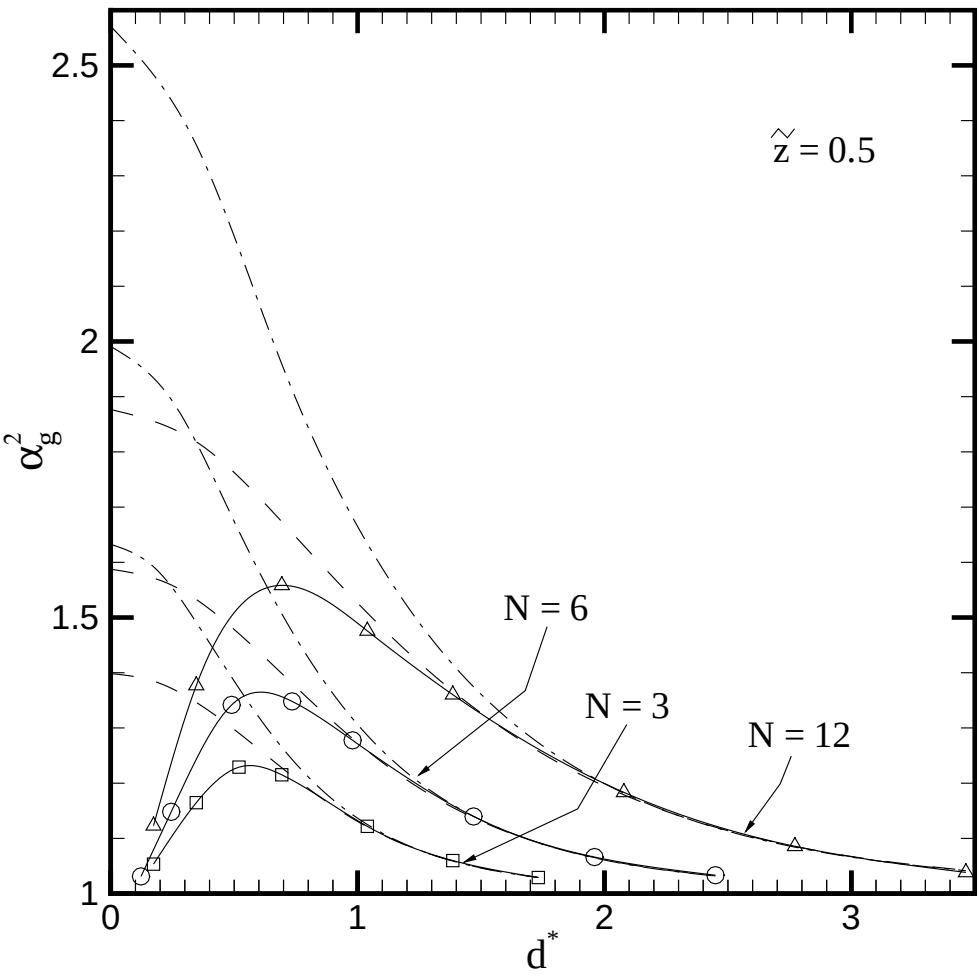

Figure 2: Swelling of the radius of gyration versus the extent of excluded volume interaction d^*, at a constant value of the strength of the interaction $\tilde{z}$, for three different values of chain length, N. Note that $\alpha_g^2 = \eta_{p,0}/\eta_{p,0}^R$. The symbols are as indicated in the caption to figure 1. The error bars in the Brownian dynamics simulations are smaller than the size of the symbols, and the continuous curves through the symbols are drawn for guiding the eye.

behavior is that, for chains of arbitrary but finite length, it is not fruitful to use a δ-function potential to represent excluded volume interactions. On the other hand, the figures seem to suggest that a finite range of excluded volume interaction is required to cause an increase from Rouse model values. Both the first order perturbation theory and the Gaussian approximation predict a significant change from Rouse model values in the limit $d^* \to 0$. In the case of a dumbbell model, we were able to rigorously understand the origin of these spurious results.[13] The incorrect term-by-term integration of a series that was not uniformly convergent was found to be the source of the problem. Since first order perturbation theory is the basis for renormalisation group calculations, the invalidity of the δ-function potential, which is frequently used in these calculations, is at first sight worrisome. However, we shall see below that the use of a δ-function potential may be legitimate when both the

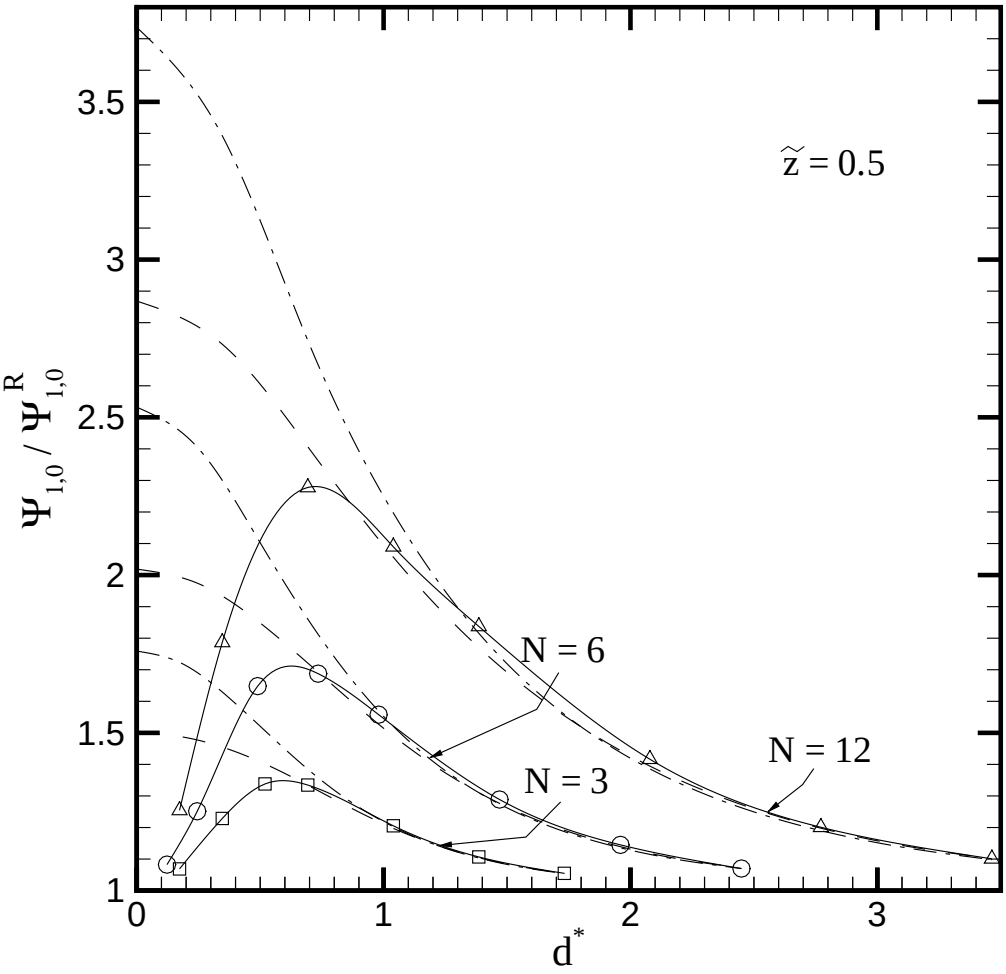

Figure 3: Ratio of the zero shear rate first normal stress difference coefficient in the presence of excluded volume interactions to the zero shear rate first normal stress difference coefficient in the Rouse model versus the extent of excluded volume interaction d^*, at a constant value of the strength of the interaction $\tilde{z}$, for three different values of chain length, N. The symbols are as indicated in the caption to figure 1. The error bars in the Brownian dynamics simulations are smaller than the size of the symbols, and the continuous curves through the symbols are drawn for guiding the eye.

limits, $N \to \infty$ and $d^* \to 0$, are considered.

Figures 1 to 3 show that there exists a threshold value of d^* at which, the results of the Gaussian approximation and the first order perturbation theory, first agree with exact Brownian dynamics simulations. This is consistent with the first order perturbation theory predictions of the end-to-end vector, equation (83), and the viscometric functions, equations (78) and (79), which reveal that, excluded volume corrections to the Rouse model decrease with increasing values of d^*. The threshold value of d^* at which the approximations become accurate, increases as N increases. This is a consequence of the well known result, which was demonstrated in section 6, that in 3 dimensions, excluded volume corrections scale as $\tilde{z}\sqrt{N}$. Note, however, that the Gaussian approximation always becomes accurate at a smaller threshold

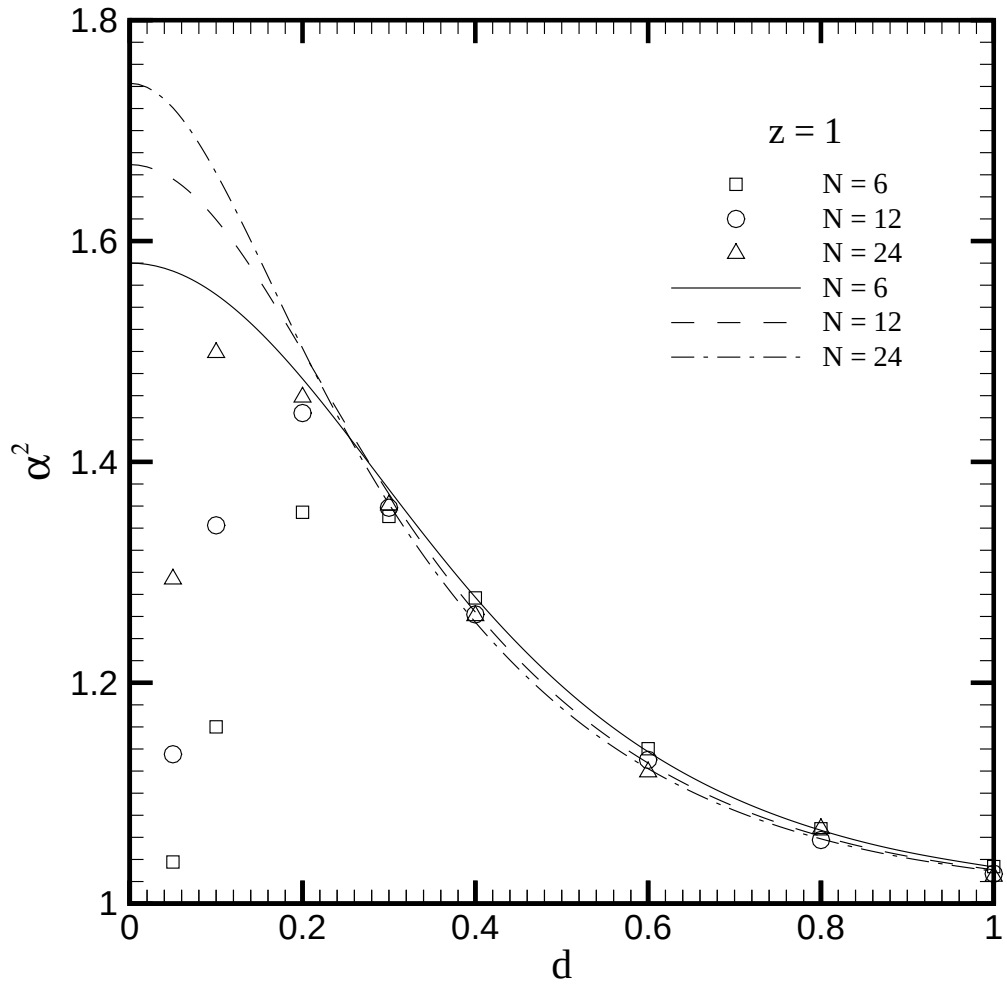

Figure 4: Equilibrium swelling of the end-to-end vector versus the extent of excluded volume interaction $d = d^*/\sqrt{N}$, at a constant value of the strength of the interaction $z = \tilde{z}\sqrt{N}$, for three different values of chain length, N. The symbols are results of Brownian dynamics simulations, while the curves are the approximate predictions of the Gaussian approximation. The error bars in the Brownian dynamics simulations are smaller than the size of the symbols.

value of d^* than the first order perturbation theory. The Gaussian approximation, while being a non-perturbative approximation, is nevertheless, exact to first order in $\tilde{z}$. Consequently, as mentioned earlier, it might be considered to consist of an infinite number of higher order terms, and can be expected to be more accurate than the results of the first order perturbation theory.

All the results in figures 1 to 3 are entirely consistent with the results obtained earlier with a dumbbell model for the polymer molecule. However, in the case of the dumbbell model, the dependence of the quality of the approximations on the chain length N, could not be examined. The results in figures 1 to 3 seem to suggest that the Gaussian approximation has a rather limited validity, since for a given value of $\tilde{z}$ and d^*, it gets progressively worse as the chain length N increases. This is in fact not a realistic picture—as is revealed below—when the data is reinterpreted in

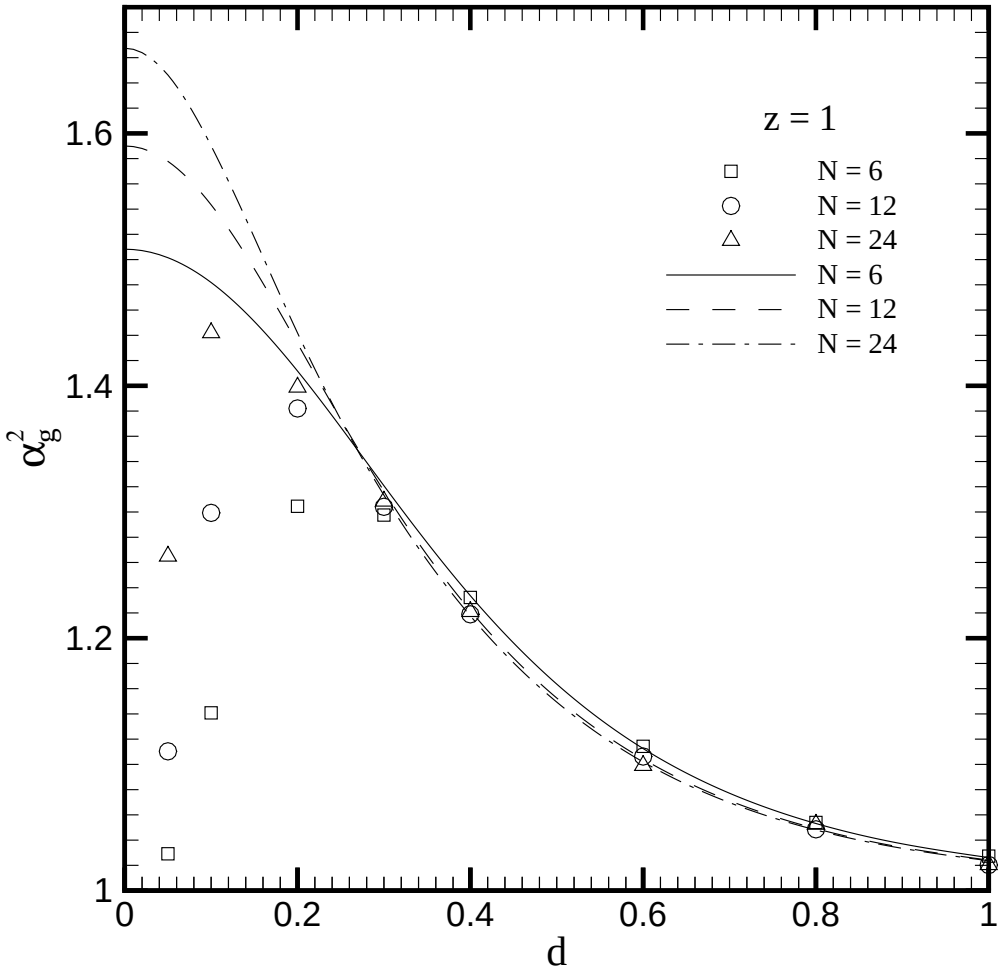

Figure 5: Swelling of the radius of gyration versus the extent of excluded volume interaction $d = d^*/\sqrt{N}$, at a constant value of the strength of the interaction $z = \tilde{z}\sqrt{N}$, for three different values of chain length, N. The symbols are results of Brownian dynamics simulations, while the curves are the approximate predictions of the Gaussian approximation. The error bars in the Brownian dynamics simulations are smaller than the size of the symbols.

terms of a different set of coordinates.

Figures 4 to 6 are plots of α^2, α_g^2 and $(\Psi_{1,0}/\Psi_{1,0}^R)$ versus $d = (d^*/\sqrt{N})$, respectively, at a constant value of $z = \tilde{z}\sqrt{N} = 1.0$, for three different chain lengths, $N = 6$, $N = 12$ and $N = 24$. Before we discuss the figures, it is appropriate to make a few remarks about the choice of the variables in terms of which the data are displayed. Firstly, we choose z as the measure of the strength of excluded volume interaction, since perturbation theory clearly reveals that in 3 dimensions, the excluded volume corrections scale as $\tilde{z}\sqrt{N}$. A constant value of z, as N increases, implies that $\tilde{z}$ must simultaneously decrease in order to keep the relative role of excluded volume interactions the same. Secondly, we choose the x-axis coordinate as $d = (d^*/\sqrt{N})$, because, as was shown in section 6, perturbation theory in the limit of long chains indicates that when the data is displayed in terms of d and z, all

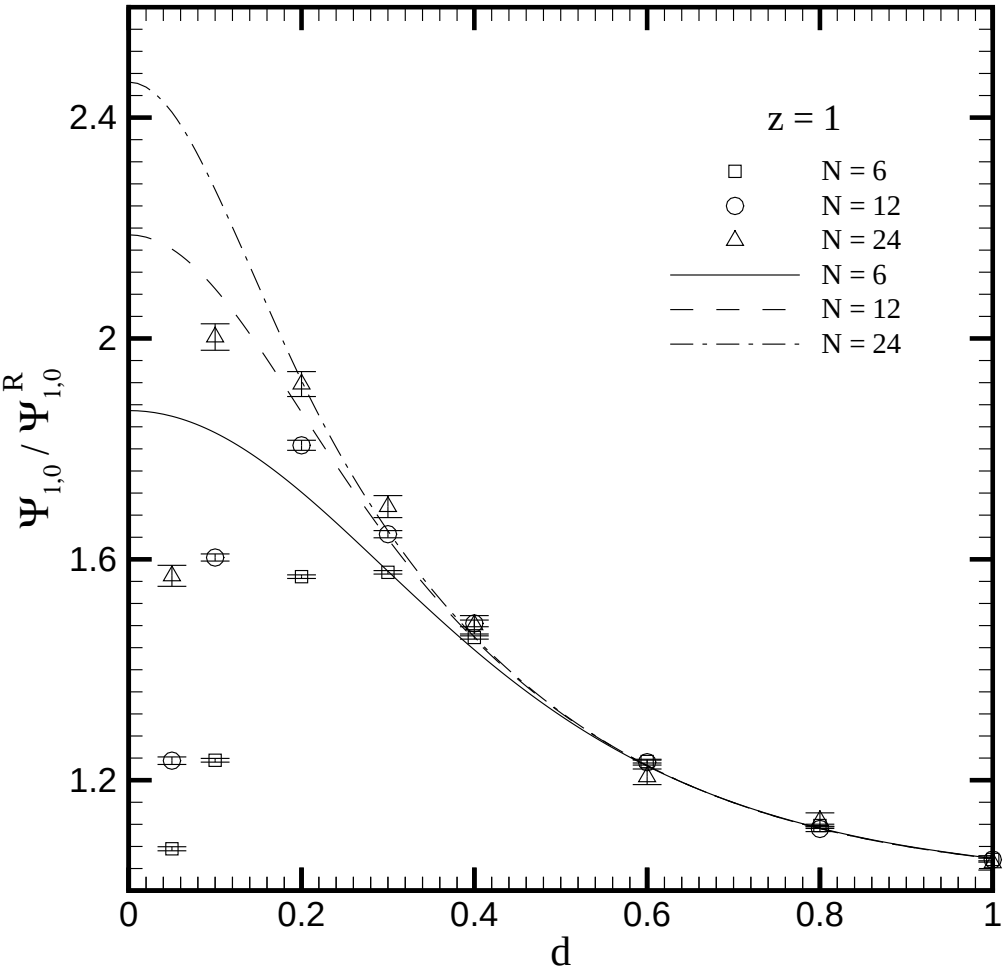

Figure 6: Ratio of the zero shear rate first normal stress difference coefficient in the presence of excluded volume interactions to the zero shear rate first normal stress difference coefficient in the Rouse model versus the extent of excluded volume interaction $d = d^*/\sqrt{N}$, at a constant value of the strength of the interaction $z = \tilde{z}\sqrt{N}$, for three different values of chain length, N. The symbols are results of Brownian dynamics simulations, while the curves are the approximate predictions of the Gaussian approximation.

the curves should collapse on to a single curve as $N \to \infty$. The parameter d may be considered to be the extent of excluded volume interaction, measured as a fraction of the unperturbed (i.e., Rouse) root mean square end-to-end vector $\sqrt{\langle \boldsymbol{r}^2 \rangle^R_{\rm eq}}$.

We first discuss the results of exact Brownian dynamics simulations displayed in figures 4 to 6. As in figures 1 to 3, all the properties start at Rouse values at $d = 0$, go through a maximum as d increases, and then finally decrease once more towards Rouse values with the continued increase of d. However, as the chain length increases, the values seem to rise increasingly more rapidly from the Rouse values at $d = 0$, towards the maximum value. In other words, the slope at the origin seems to be getting steeper as N increases. Indeed, the trend of the data leads one to speculate that, in the limit $N \to \infty$, the data might be singular at $d = 0$,

and consequently legitimise, in this limit, the use of a δ-function excluded volume potential. This conclusion is of course only speculative, and needs to be established more rigorously. It has not been possible to examine more closely, with the help of Brownian dynamics simulations, the behavior at small values of d for larger values of N, because of the excessive CPU time that is required. In terms of the non-dimensional time $t^* = (t/\lambda_H)$, a run for two non-dimensional time steps $\Delta t^* = 0.1$ and $\Delta t^* = 0.08$, took roughly 51 hours of CPU time on a SGI o2000, for $N = 24$.

When viewed in terms of z and d, the Gaussian approximation is revealed to be far more satisfactory than appeared at first sight in figures 1 to 3. Indeed, for relatively small values of d, where the Gaussian approximation is inaccurate at small values of chain length, the Gaussian approximation seems to be becoming more accurate as N increases. One might expect that as $N \to \infty$, the Gaussian approximation becomes accurate for an increasingly larger range of d values. However, as will perhaps become clearer with the results discussed below, it appears that, for a given value of z, there exists a threshold value of d, *below* which the Gaussian approximation will be *inaccurate*, no matter how large a choice of N is made. The reason for this behavior is related to a feature that is just noticeable in these figures—curves for different values of N appear to be converging to an asymptote. This feature will become much clearer in figure 7, and will be discussed in greater detail below.

For the sake of clarity, the predictions of the first order perturbation theory are not displayed in figures 4 to 6. In contrast to the situation in figures 1 to 3, where the accuracy of the first order perturbation theory becomes progressively worse as N increases, its accuracy appears *frozen* when viewed in terms of z and d. In other words, for different—sufficiently large—values of N, the first order perturbation theory first becomes accurate at the same threshold value of d. As in the case of the predictions of the Gaussian approximation, curves for different values of N appear to be converging to a common asymptote. This can be seen clearly in figure 7.

Figure 7 displays plots of α^2 versus d, for different chain lengths, at a constant value of $z = 1$. It clearly reveals the fact that, both in the Gaussian approximation and in the first order perturbation theory, curves for different values of N collapse on to a single curve in the limit $N \to \infty$. A similar approach to an asymptotic limit is observed as $N \to \infty$, in the predictions of α_g^2 and $(\Psi_{1,0}/\Psi_{1,0}^R)$ by both the approximations, when they are plotted versus d. The results of Brownian dynamics simulations for $N = 24$ are also plotted in figure 7. They indicate that for $z = 1$, asymptotic values have already been reached by Brownian dynamics simulations, at this relatively small value of N, for $d \geq 0.3$. One expects that as N increases, asymptotic values will be reached for smaller and smaller values of d.

The asymptotic values predicted by the first order perturbation theory were obtained by carrying out the integrals in equation (85) analytically. It is worth noting that the convergence to the asymptotic value is quite slow as $d \to 0$. On the other hand, the asymptotic values predicted by the Gaussian approximation were obtained by a numerical procedure, as discussed below.

In the Gaussian approximation, calculation of the equilibrium and zero shear

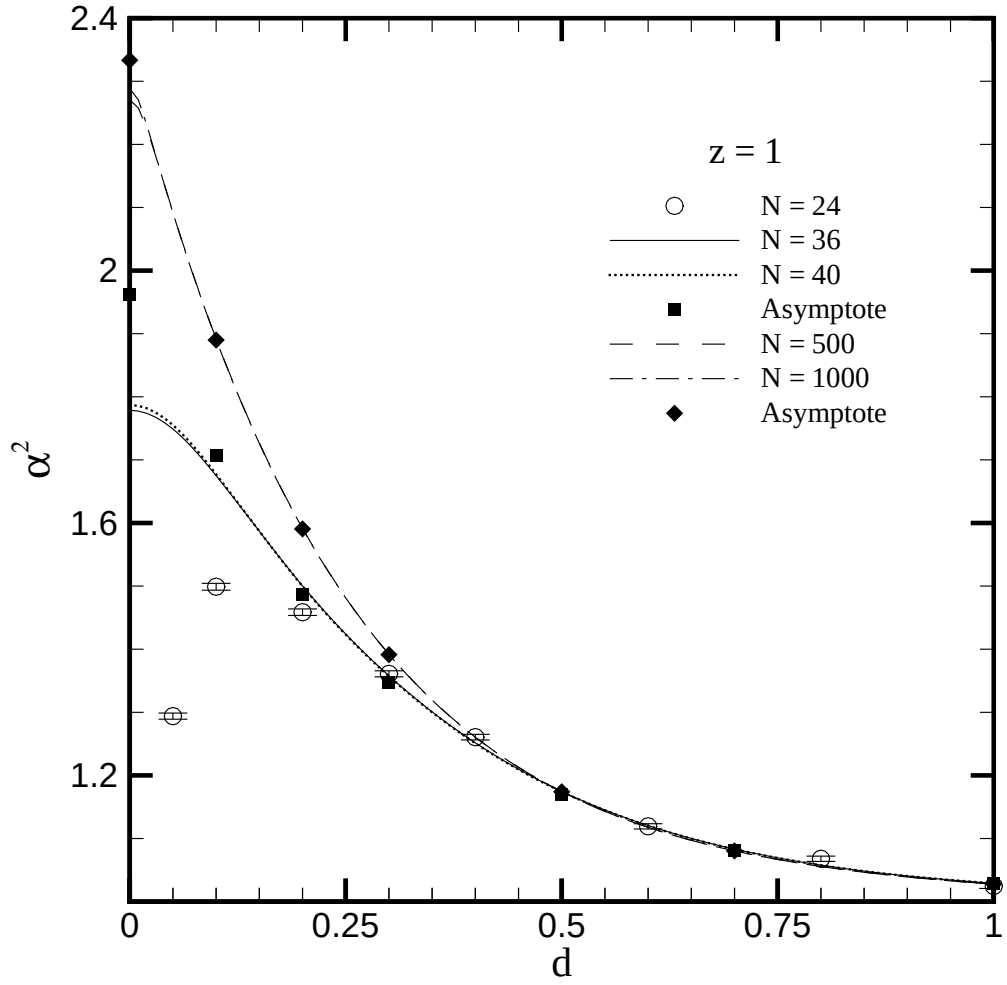

Figure 7: Equilibrium swelling of the end-to-end vector versus d, at a constant value of z, for different N. The continuous and dotted curves are the predictions of the Gaussian approximation. The filled squares are the asymptotic predictions of the Gaussian approximation, obtained by numerical extrapolation of finite chain data to the limit of infinite chain length. The dashed and dot-dashed curves are the predictions of the first order perturbation theory. The filled diamonds are the predictions of the first order perturbation theory in the long chain limit, obtained by carrying out the integrals in equation (85) analytically. The circles, with error bars, are the results of Brownian dynamics simulations for $N = 24$.

rate quantities requires the evaluation of the equilibrium moments f_{jk}. These are found here, as mentioned earlier, by numerical integration of the system of ordinary differential equations, equation (46), using a simple Euler scheme, until steady state is reached. In addition, the evaluation of $\eta_{p,0}$ and $\Psi_{1,0}$ requires the inversion of the $(N-1)^2 \times (N-1)^2$ matrix $\overline{A}_{jk,mn}$. As a result, the CPU time scales as N^6, and makes the task of generating data for large values of N extremely computationally intensive. We have explored the predictions of chains up to a maximum of $N = 40$, since for this value of N, a single run on a SGI o2000 computer took approximately 54 hours of CPU time. The asymptotic values in figure 7 were obtained by the following procedure. For $z = 1$, equilibrium and zero shear rate data, consisting of

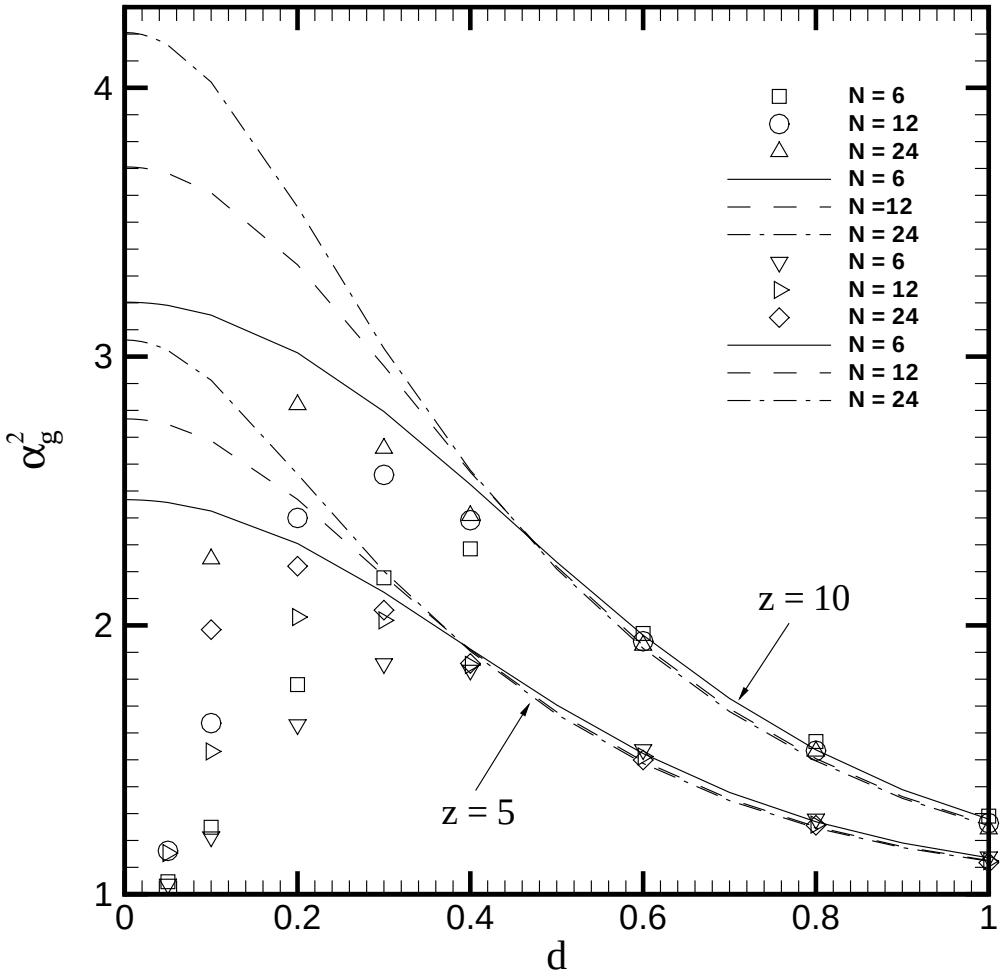

Figure 8: Swelling of the radius of gyration versus d, at two values of z, for three different values of N. The symbols are results of Brownian dynamics simulations, while the curves are the approximate predictions of the Gaussian approximation. The error bars in the Brownian dynamics simulations are smaller than the size of the symbols.

property values at different pairs of values (d, N), were first compiled by performing a large number of runs for various values of N as a function of d. A specific value of d was then chosen, and assuming that the various properties were functions of $1/\sqrt{N}$, the values for different N were extrapolated to the limit $N \to \infty$ using a rational function extrapolation algorithm.[14] The choice of $\sqrt{N}$ is motivated by the fact that the leading correction to the integrals in equation (85), is of order $N^{-1+\epsilon/2}$.[17]

The quality of Gaussian approximation as a function of the variable z, for the quantities α_g^2 and $(\Psi_{1,0}/\Psi_{1,0}^R)$, is displayed in figures 8 and 9, respectively. The behavior of α^2 has not been displayed as it is very similar to that of α_g^2. It is clear from these figures that for a given value of N, the threshold value of d beyond which the Gaussian approximation is accurate increases as z increases. On the other hand, as in the case of $z = 1$, for a fixed value of z, the accuracy of the Gaussian approximation seems to be increasing with N, for small values of d. There

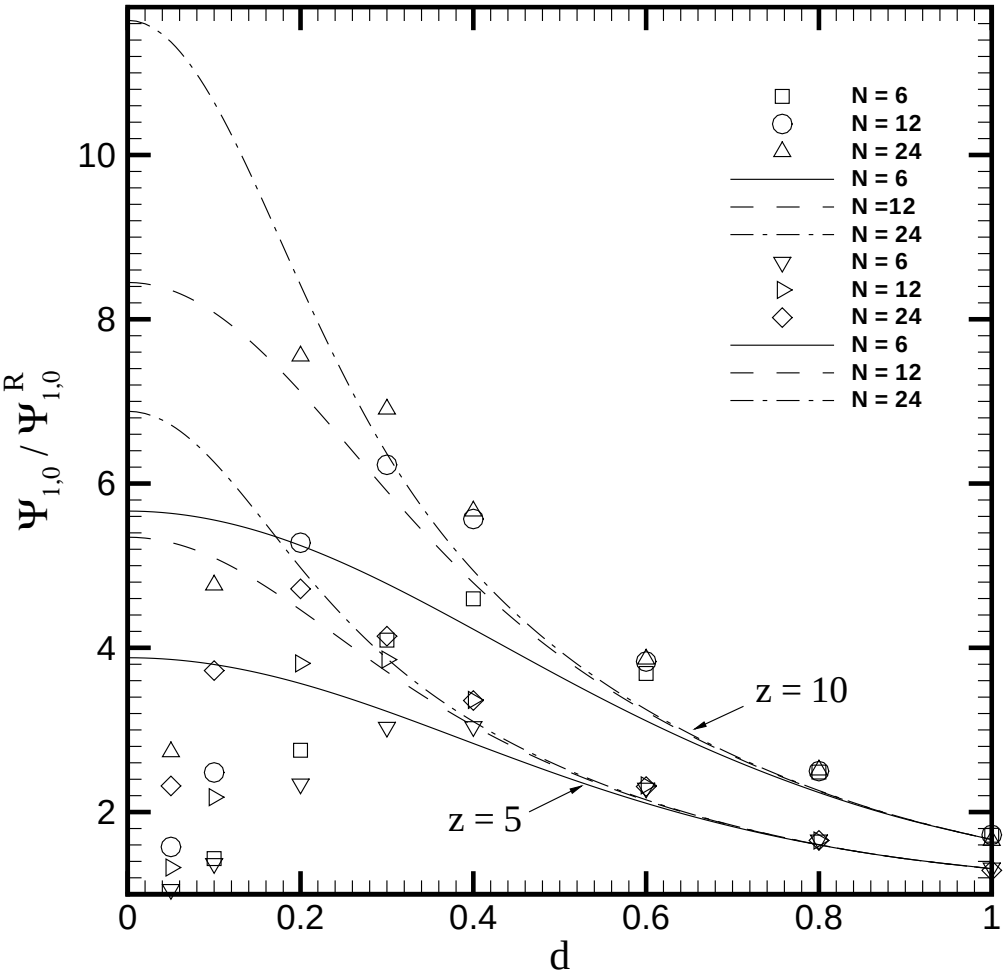

Figure 9: Ratio of the zero shear rate first normal stress difference coefficient in the presence of excluded volume interactions to the zero shear rate first normal stress difference coefficient in the Rouse model versus d, at two values of z, for three different values of N. The symbols are results of Brownian dynamics simulations, while the curves are the approximate predictions of the Gaussian approximation.

is, however, clearly a limit to this accuracy. As N becomes large, the results of the exact Brownian dynamics simulations and the Gaussian approximation approach asymptotic values, and consequently, no further change can be noticed with changing N. Figures 8 and 9 seem to indicate that at small values of d, while the asymptotic values of Brownian dynamics simulations lie *below* the asymptotic values of the Gaussian approximation for α_g^2, the opposite is true for $(\Psi_{1,0}/\Psi^R_{1,0})$. A clearer picture would be obtained if it were possible to carry out Brownian dynamics simulations with larger values of N.

We now examine the approach to *universality* in the predictions of the Gaussian approximation. The renormalisation group analysis arguments in section 6 indicate that for large values of the parameter z, one would expect the scaling with molecular weight, of various observable quantities, to become independent of d. A similar

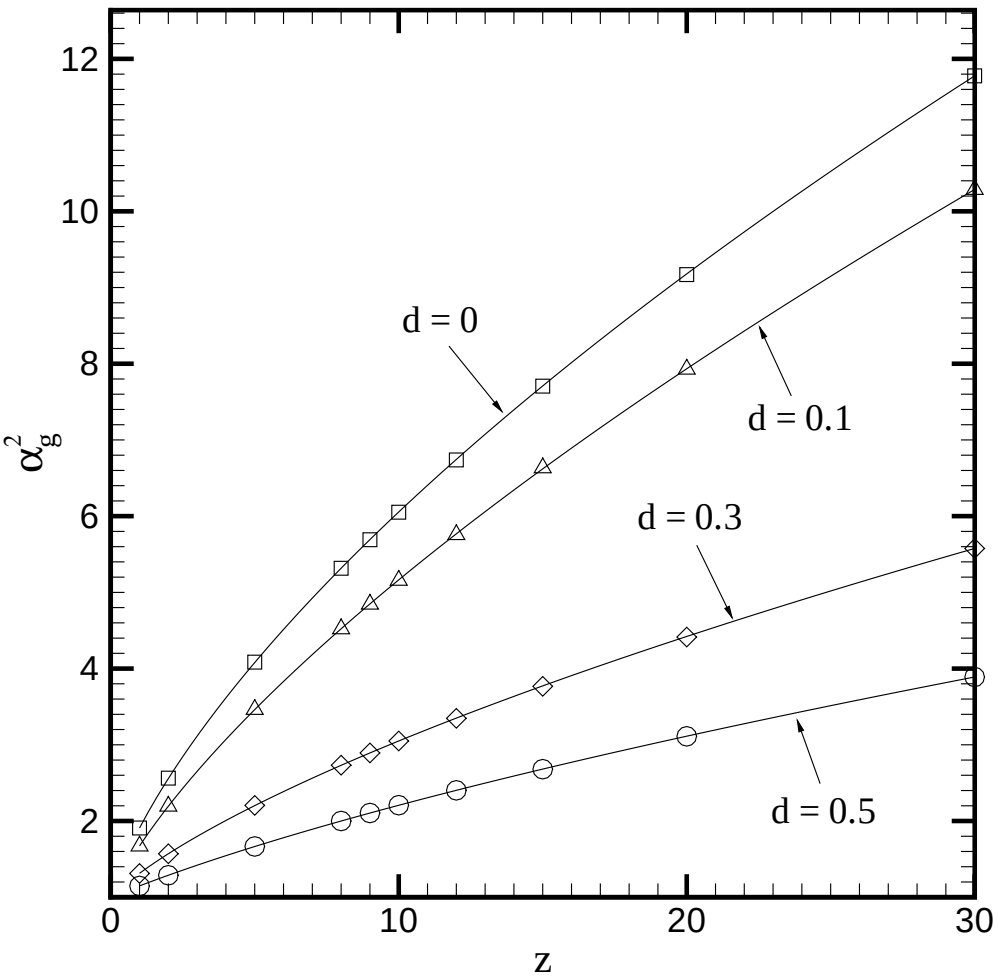

Figure 10: Asymptotic swelling of the radius of gyration versus z, at various values of d. The symbols are the results of the Gaussian approximation, while the lines are curve fits using an equation of the form (97). The curve fit parameters are given in Table 3.

behavior is expected of non-dimensional ratios constructed with these quantities. The symbols in figures 10 and 11 are *asymptotic* predictions of α_g^2 and $(\Psi_{1,0}/\Psi_{1,0}^R)$ by the Gaussian approximation, plotted as a function of z for four different values of d. The behavior of α^2 has not been displayed as it is very similar to that of α_g^2. At each value of z, the asymptotic values were obtained by the numerical extrapolation procedure discussed above in the context of figure 7. The lines through the symbols are curve fits, using an equation which has a form commonly used to fit results of renormalisation group analysis,[17]

$$y = \left(1 + a\,z + b\,z^2\right)^m \tag{97}$$

where, y represents the fitted variable. The parameters a, b and m, for α^2, α_g^2 and $(\Psi_{1,0}/\Psi_{1,0}^R)$, are given in Table 3. The maximum difference between the computed data and the curve fit for all the three properties was less than 1.3%.

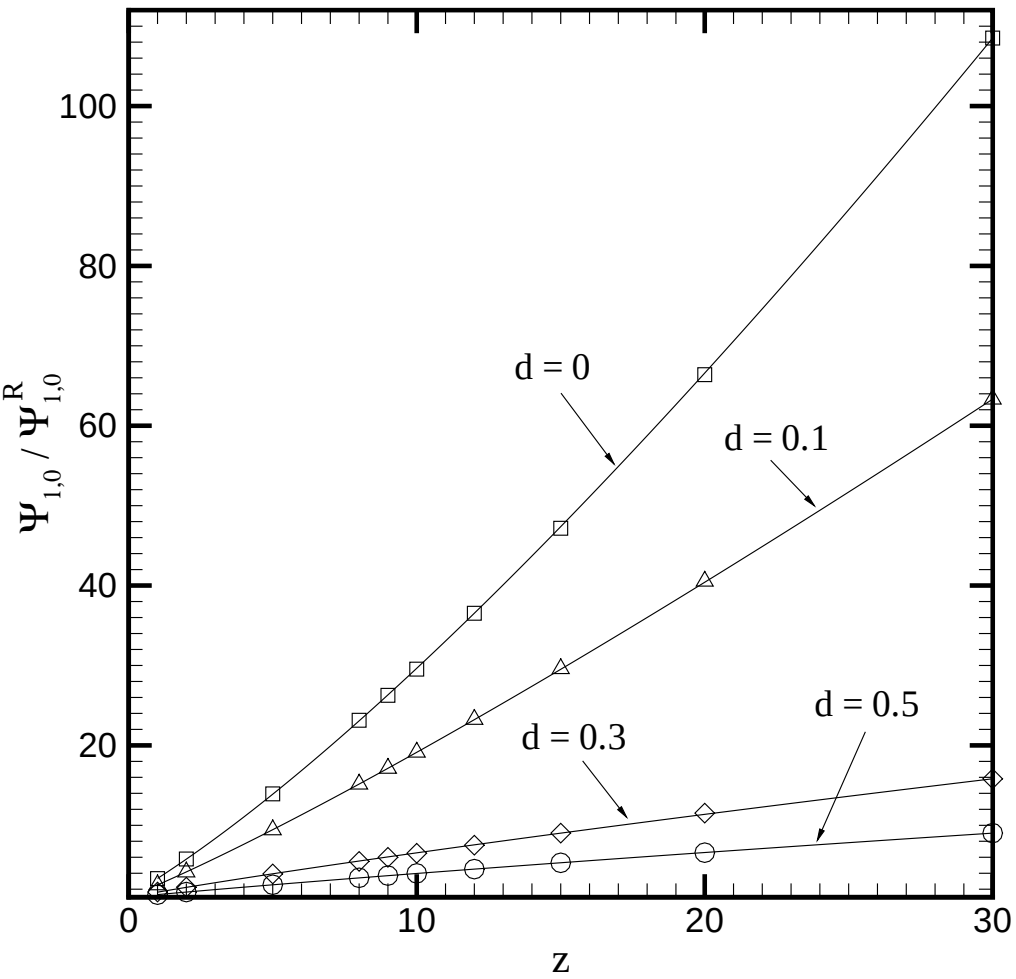

Figure 11: Asymptotic ratio of the zero shear rate first normal stress difference coefficient in the presence of excluded volume interactions to the zero shear rate first normal stress difference coefficient in the Rouse model versus z, at various values of d. The symbols are the results of the Gaussian approximation, while the lines are curve fits using an equation of the form (97). The curve fit parameters are given in Table 3.

The N dependence of the equilibrium properties $\langle \boldsymbol{r}^2 \rangle_{\rm eq}$ and $\langle R_g^2 \rangle_{\rm eq}$, for large values of N, can be obtained from equation (97), and the definitions of the quantities α^2 and α_g^2. Both the properties scale identically with molecular weight, namely, as $N^{2\nu}$. Experimental results suggest a value of $\nu = 0.592 \pm 0.003$,[6] while renormalisation group calculations and Monte Carlo simulations suggest a value of $\nu = 0.588$.[5,17] Since z scales as $N^{1/2}$, it is clear from equation (97) that for large values of N, $\nu = (1+m)/2$. From Table 3, one can see that the values of m for α^2 and α_g^2, for all the values of d, are within 6% of each other, i.e. they are nearly independent of d, and imply a Gaussian approximation prediction of ν between 0.659 and 0.668. It must be noted, however, that this is the implication of data accumulated up to $z = 30$. At this value of z, the data might still only reflect the crossover region between Rouse scaling and the final scaling in the 'excluded volume limit' of large z.

Table 3: Parameters appearing in equation (97), used to fit the asymptotic predictions of the Gaussian approximation, displayed in figures 10 and 11.

	α^2			α_g^2			$(\Psi_{1,0}/\Psi_{1,0}^R)$		
d	a	b	m	a	b	m	a	b	m
0	4.352	2.715	0.323	4.178	2.453	0.318	4.058	1.755	0.630
0.1	2.310	1.635	0.328	2.569	1.057	0.336	2.640	1.421	0.575
0.3	1.193	0.263	0.333	1.154	0.212	0.317	0.736	-0.0009	0.890
0.5	0.516	0.083	0.333	0.483	0.060	0.320	0.377	-0.0005	0.889

As a result, the curve fit parameter m might change as data is compiled for larger values of z. The problem with going to larger values of z is that in order to maintain the accuracy of the numerical extrapolation procedure, one must have data for values of $N > 40$, which, as was mentioned earlier, requires large amounts of CPU time. In the treatment of the non-linear microscopic phenomenon of hydrodynamic interaction, the development of an alternative approximation to the Gaussian approximation, which was as accurate but significantly less computationally intensive, enabled the examination of chains with lengths up to $N = 100$.[12]

While the values of m for α^2 and α_g^2 are close to each other for all the values of d—in line with our expectations—the values of m for the ratio $(\Psi_{1,0}/\Psi_{1,0}^R)$ are significantly different at $d = 0$ and $d = 0.1$ from those at $d = 0.3$ and $d = 0.5$. We expect the value of m for $(\Psi_{1,0}/\Psi_{1,0}^R)$ to be twice the value of m for α_g^2. This follows from equation (96), since $\Psi_{1,0}$ scales as $\eta_{p,0}^2$, and $\eta_{p,0}^R$ and $\Psi_{1,0}^R$ scale with N as N^2 and N^4, respectively. It is felt that this discrepancy is again a reflection of the data being in the cross over region. There is evidence for this point of view from the results displayed in figures 12 and 13.

Figures 12 and 13 examine the z dependence of two non-dimensional ratios predicted by the Gaussian approximation, for various values of d.[15] These ratios are defined by,

$$U_R = 6\,\frac{\langle R_g^2 \rangle_{\rm eq}}{\langle \boldsymbol{r}^2 \rangle_{\rm eq}}\,; \quad U_{\Psi\eta} = \frac{n_{\rm p} k_{\rm B} T \Psi_{1,0}}{\eta_{p,0}^2} \tag{98}$$

Though all the curves in figures 12 and 13 decrease relatively rapidly for small values of z, and appear to be levelling off as z increases, they still have negative slopes at

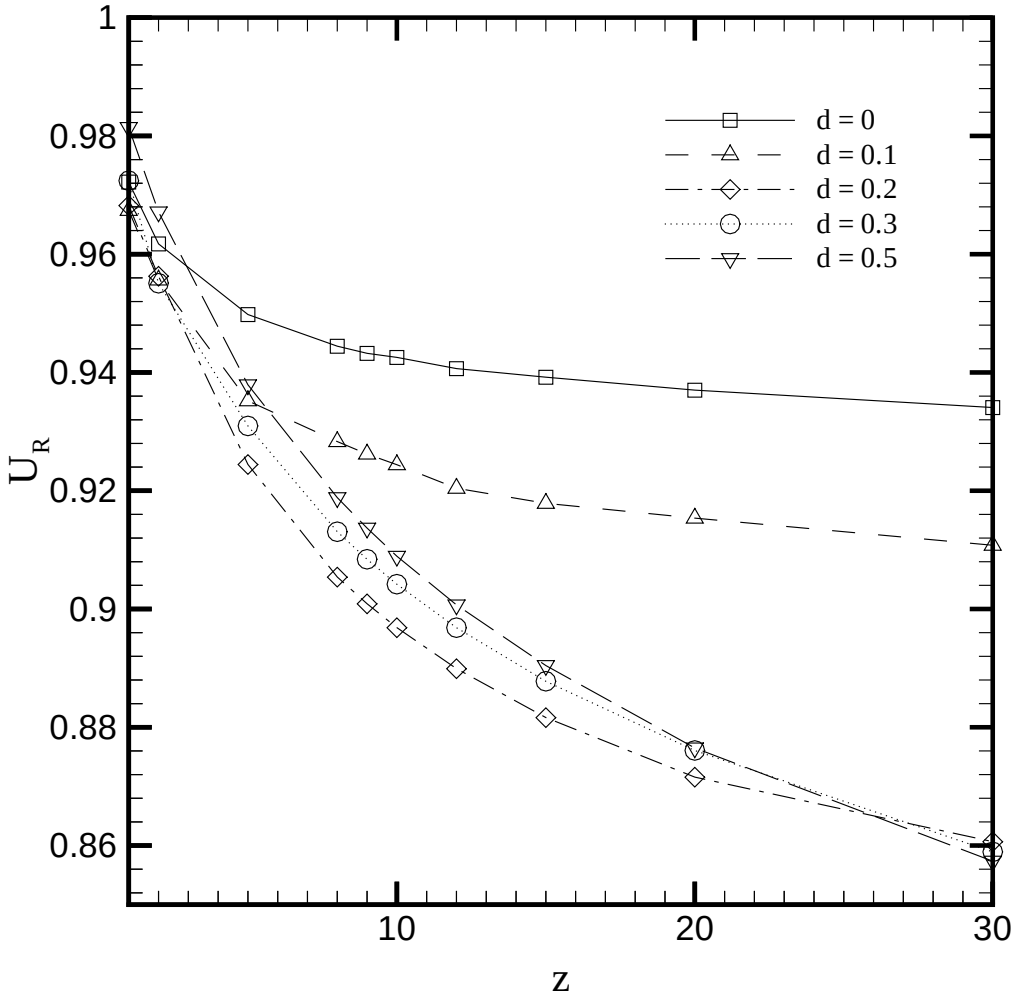

Figure 12: Universal ratio constructed from the radius of gyration and the end-to-end vector versus z, at various values of d. The symbols are the results of the Gaussian approximation, while the lines are drawn to guide the eye.

$z = 30$. This suggests that the asymptotic values of the ratios at large values of z are yet to be reached, and the data reflects behavior in the cross over regime rather than in the excluded volume limit.

In the Rouse model, $U_R = 1$. Both renormalisation group calculations and Monte Carlo simulations yield an identical value of $U_R = 0.959$ in the excluded volume limit.[17] Though the curves in figure 12 have not yet levelled off to a constant value independent of z, it is already apparent that the Gaussian approximation predicts a smaller value of U_R in the limit of large z. The most note worthy feature is that the curves for $d = 0.2$, 0.3 and 0.5, are beginning to merge together as z increases, justifying the expectation that universal ratios should be independent of the choice of d. The curves for $d = 0$ and 0.1 are significantly apart from these curves. They appear to be levelling off to a constant value, but whether they ultimately approach the same limiting value as for larger values of d, cannot be decided based on the present range of data. It is also perhaps relevant here to point out that

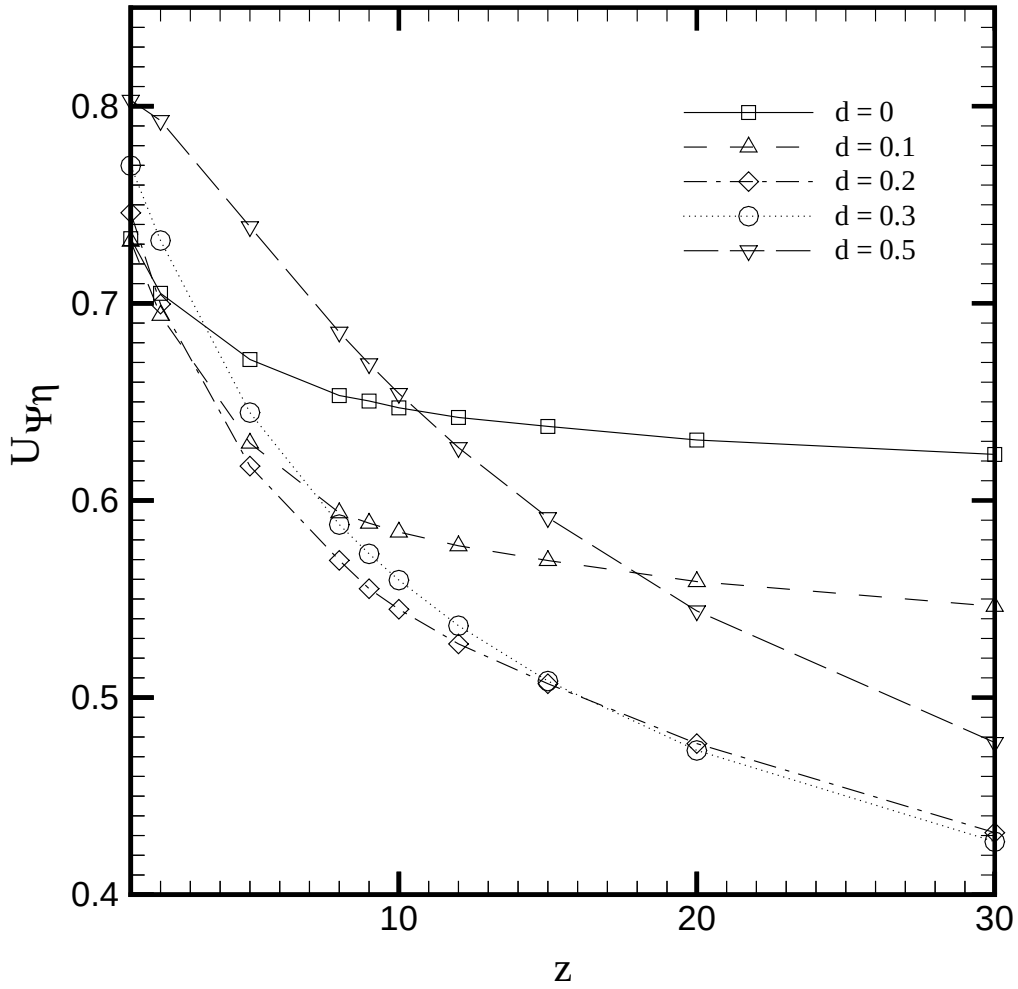

Figure 13: Universal ratio constructed from the zero shear rate first normal stress difference coefficient and the zero shear rate viscosity versus z, at various values of d. The symbols are the results of the Gaussian approximation, while the lines are drawn to guide the eye.

the convergence, at fixed values of z and d, to asymptotic values for $N \to \infty$, gets increasingly slower as $d \to 0$.

For long chains, $U_{\Psi\eta} = 0.8$ in the Rouse model, while a renormalisation group calculation yield a value $U_{\Psi\eta} = 0.6288$.[9] It is clear from the curves for $d = 0.1$, 0.2, 0.3 and 0.5 in figure 13, that the Gaussian approximation predicts a smaller value of $U_{\Psi\eta}$ in the limit of large z. Curiously, the value of $U_{\Psi\eta}$ for $d = 0$, at $z = 30$, is close to the prediction of the renormalisation group calculation. As in the case of the ratio U_R, the curves for $d = 0.2$ and 0.3 merge together as z increases, and the curve for $d = 0.5$ seems to be tending to the same asymptotic value. The curves for $d = 0$ and 0.1 are again significantly apart, and their ultimate asymptotic behavior cannot be decided based on the present range of data.

8 Conclusions

The influence of excluded volume interactions on the linear viscoelastic properties of a dilute polymer solution has been studied with the help of a narrow Gaussian excluded volume potential that acts between pairs of beads in a bead-spring chain model for the polymer molecule. Exact predictions of the model have been obtained by carrying out Brownian dynamics simulations, and approximate predictions have been obtained by two methods—firstly, by carrying out a first order perturbation expansion in the strength of excluded volume interaction, and secondly, by introducing a Gaussian approximation for the configurational distribution function.

The most appropriate way to represent the results of model calculations has been shown to be in terms of a suitably normalised strength of excluded volume interaction z, and a suitably normalised extent of excluded volume interaction d. When the results are viewed in terms of these variables, the following conclusions can be drawn:

1. The use of a δ-function excluded volume potential (which is the narrow Gaussian excluded volume potential in the limit $d \to 0$) is not fruitful for chains with an arbitrary, but finite, number of beads N, because it leads to the prediction of properties identical to the Rouse model. The narrow Gaussian potential with a finite, non-zero, extent of interaction d, on the other hand, causes a swelling of the polymer chain at equilibrium, and an increase in the zero shear rate properties from their Rouse model values.

2. Curves for different—but sufficiently large—values of chain length N, collapse on to a unique asymptotic curve in the limit $N \to \infty$. The manner in which the results of Brownian dynamics simulations approach the asymptotic behavior indicates that there might be a singularity at $d = 0$, and consequently, the use of a δ-function excluded volume potential might be justified in the limit of infinite chain length.

3. The accuracy of the first order perturbation expansion becomes independent of N for large N. For a given value of z, there exists a threshold value of d beyond which the results of the first order perturbation theory agree with the exact results of Brownian dynamics simulations.

4. As in the case of the first order perturbation expansion, there exists a threshold value of d beyond which the results of the Gaussian approximation agree with exact results. For a given value of z, this threshold value for accuracy is smaller than the threshold value in the first order perturbation theory. The accuracy of the Gaussian approximation decreases with increasing values of z.

There are two significant benefits gained by carrying out the first order perturbation theory. Firstly, the development of explicit expressions for the end-to-end vector and the viscometric functions in terms of the model parameters, enables one to understand the behavior of the Gaussian approximation. This is because the

Gaussian approximation is shown here to be exact to first order in z. Secondly, the results of the first order perturbation theory may be refined by using renormalisation group arguments to understand the role of the parameter d.

Renormalisation group arguments, carried out in the context of the end-to-end vector at equilibrium, seem to suggest that the scaling with molecular weight of the equilibrium and zero shear rate properties, and the values of non-dimensional ratios of these quantities, should become independent of d in the excluded volume limit of large z. The asymptotic results of the Gaussian approximation have been examined in the light of these expectations. While some of the data does indicate independence from the choice of d, it seems likely that the present data describes the cross over region, and that it is necessary to generate data at larger values of z (and consequently N) before firm conclusions can be drawn. A barrier to such computations is the computational intensity of the Gaussian approximation, which scales as N^6.

The accuracy of the Gaussian approximation, for a given value of z and d, is expected to improve as the shear rate increases. This follows from the fact that corrections to the Rouse model, due to excluded volume interactions, decrease with increasing shear rate. Viscometric functions predicted by Brownian dynamics simulations, the Gaussian approximation, and the first order perturbation expansion in 3 dimensions, will be compared in a subsequent publication.

The Gaussian approximation has been shown to be an excellent approximation for the treatment of hydrodynamic interactions. In this paper we have seen that it is also a good approximation for describing excluded volume interactions, albeit within a certain range of parameter values. It would be interesting to examine the quality of the Gaussian approximation in a model for the combined effects of hydrodynamic interaction and excluded volume.

Acknowledgement. Support for this work through a grant III. 5(5)/98-ET from the Department of Science and Technology, India, is acknowledged. A significant part of this work was carried out while the author was an Alexander von Humboldt fellow at the Department of Mathematics, University of Kaiserslautern, Germany. The author would also like to thank the High Performance Computational Facility at the University of Kaiserslautern, and Professor H. C. Öttinger, for providing the use of their computers.

References

[1] Bird, R. B.; Armstrong, R. C.; Hassager, O. *Dynamics of Polymeric Liquids. Fluid Mechanics,* 2nd edn.; Wiley-Interscience: New York, 1987; Vol. 1.

[2] Bird, R. B.; Curtiss, C. F.; Armstrong, R. C.; Hassager, O. *Dynamics of Polymeric Liquids. Kinetic Theory,* 2nd edn.; Wiley-Interscience: New York, 1987; Vol. 2.

[3] des Cloizeaux, J.; Jannink, G. *Polymers in Solution, Their Modelling and Structure*; Oxford University Press: Oxford, 1990.

[4] Doi, M.; Edwards, S. F. *The Theory of Polymer Dynamics*; Oxford University Press: Oxford, 1986.

[5] Graessley, W. W.; Hayward, R. C.; Grest, G.S. *Macromolecules* **1999**, 32, 3510.

[6] Hayward, R. C.; Graessley, W. W. *Macromolecules* **1999**, 32, 3502.

[7] Öttinger, H. C. *J. Chem. Phys.* **1989**, 90, 463.

[8] Öttinger, H. C.; Rabin, Y. *J. Non-Newtonian Fluid Mech.* **1989**, 33, 53.

[9] Öttinger, H. C. *Phys. Rev.* **1989**, A40, 2664.

[10] Öttinger, H. C. *Stochastic Processes in Polymeric Fluids*; Springer: Berlin, 1996.

[11] Prakash, J. R. 'The Kinetic Theory of Dilute Solutions of Flexible Polymers: Hydrodynamic Interaction'; In *Advances in the Flow and Rheology of Non-Newtonian Fluids*; Siginer, D. A.; Kee, D. De; Chhabra, R. P.; Eds; Rheology Series; Elsevier Science: Amsterdam, 1999.

[12] Prakash, J. R.; Öttinger, H. C. *J. Non-Newtonian Fluid Mech.* **1997**, 71, 245.

[13] Prakash, J. R.; Öttinger, H. C. *Macromolecules* **1999**, 32, 2028.

[14] Press, W. H.; Teukolsky, S. A.; Vetterling, W. T.; Flannery, B. P. *Numerical Recipes in FORTRAN*, 2nd edn.; Cambridge University Press: Cambridge, 1992.

[15] The non-dimensional ratio, $U_{\eta R} = \left[\eta_{p,0}/n_{\rm p}\eta_s(4\pi/3)\langle R_g^2\rangle_{\rm eq}^{3/2}\right]$, is not a universal ratio in the present model since it scales with N as $N^{1-\nu}$. It becomes a universal ratio only when hydrodynamic interaction effects are included in the model.

[16] Rouse, P.E.; *J. Chem. Phys.* **1953**, 21, 1272.

[17] Schäfer, L. *Excluded Volume Effects in Polymer Solutions*; Springer: Berlin, 1999.

[18] Schieber, J. D.; *J. Rheol.* **1993**, 37, 1003.

[19] Wagner, N. J.; Öttinger, H. C. *J. Rheol.* **1997**, 41, 757.

[20] Wedgewood, L. E. *J. Non-Newtonian Fluid Mech.* **1989**, 31, 127.

[21] Wedgewood, L. E. *Rheol. Acta* **1993**, 32, 405.

[22] Zylka, W. *J. Chem. Phys.* **1991**, 94, 4628.

[23] Zylka, W.; Öttinger H. C. *Macromolecules* **1991**, 24, 484.

A $P_{\rm eq}(\boldsymbol{r}_{\nu\mu})$ in the limit $\tilde{d} \to 0$ or $\tilde{d} \to \infty$

Upon substituting equation (14) and the Fourier representation of a δ-function into equation (30), and rearranging terms, one obtains,

$$P_{\rm eq}(\boldsymbol{r}_{\nu\mu}) = \frac{1}{(2\pi)^3} \int d\boldsymbol{k}\, e^{i\,\boldsymbol{r}_{\nu\mu}\cdot\boldsymbol{k}} \left\{ \mathcal{N}_{\rm eq} \int d\boldsymbol{Q}_1 \ldots d\boldsymbol{Q}_{N-1}\, e^{-\left[(\phi/k_{\rm B}T)+i\left(\sum_{j=\mu}^{\nu-1}\boldsymbol{Q}_j\right)\cdot\boldsymbol{k}\right]} \right\} \tag{99}$$

We now consider the integral within braces on the right hand side of equation (99), and take up the integration over the bead connector vector $\boldsymbol{Q}_1$. Separating out all the terms containing the vector $\boldsymbol{Q}_1$, we can rewrite this integral as,

$$\begin{aligned} \mathcal{N}_{\rm eq} \int d\boldsymbol{Q}_2 \ldots d\boldsymbol{Q}_{N-1}\, \exp\Big[& -\frac{H}{2k_{\rm B}T} \sum_{j=2}^{N-1} \boldsymbol{Q}_j^2 - i \left(\sum_{j=\mu}^{\nu-1} (1-\delta_{1j})\, \boldsymbol{Q}_j \right) \cdot \boldsymbol{k} \\ & - \frac{1}{2k_{\rm B}T} \sum_{\substack{\alpha,\beta=2 \\ \alpha\neq\beta}}^{N} E\left(\boldsymbol{r}_\alpha - \boldsymbol{r}_\beta\right) \Big] \left\{ \int d\boldsymbol{Q}_1\, \exp\Big[-\frac{H}{2k_{\rm B}T}\, \boldsymbol{Q}_1^2 - i\,\delta_{1\mu}\, \boldsymbol{Q}_1 \cdot \boldsymbol{k} \right. \\ & \left. - \frac{1}{k_{\rm B}T} \left[E\left(\boldsymbol{r}_1 - \boldsymbol{r}_2\right) + E\left(\boldsymbol{r}_1 - \boldsymbol{r}_3\right) + \ldots + E\left(\boldsymbol{r}_1 - \boldsymbol{r}_N\right) \right] \Big] \right\} \end{aligned} \tag{100}$$

where, a typical term of the excluded volume potential contribution to the $\boldsymbol{Q}_1$ integral, has the form,

$$\begin{aligned} E\left(\boldsymbol{r}_1 - \boldsymbol{r}_\beta\right) \;=\; & \frac{v\, k_{\rm B}T}{\left[2\pi\tilde{d}^2\right]^{\frac{3}{2}}} \exp\Big\{ -\frac{1}{2\tilde{d}^2} \Big(\boldsymbol{Q}_1^2 + 2\,\boldsymbol{Q}_1\cdot\boldsymbol{r}_{\beta 2} + \boldsymbol{Q}_2^2 + 2\,\boldsymbol{Q}_2\cdot\boldsymbol{r}_{\beta 3} + \ldots \\ & + \boldsymbol{Q}_{\beta-2}^2 + 2\,\boldsymbol{Q}_{\beta-2}\cdot\boldsymbol{r}_{\beta,\beta-1} + \boldsymbol{Q}_{\beta-1}^2 \Big) \Big\} \end{aligned}$$

We now convert the $\boldsymbol{Q}_1$ integral into spherical coordinates. In order to do so, we need to choose a reference vector to fix a direction in space. In the $\boldsymbol{Q}_1$ integration, all the other vectors, $\boldsymbol{Q}_2, \ldots, \boldsymbol{Q}_{N-1}$ and $\boldsymbol{k}$ are fixed. Without loss of generality, we choose the fixed vector as $\boldsymbol{Q}_2$, denote its direction as the z direction, and choose, in the plane perpendicular to $\boldsymbol{Q}_2$, an arbitrary pair of orthogonal directions as the x and y axes. Let, θ_1, $\theta_{\beta 2}$, and θ_k represent the angles that the vectors $\boldsymbol{Q}_1$, $\boldsymbol{r}_{\beta 2}$ and $\boldsymbol{k}$ make with the z direction, respectively. Similarly, let ϕ_1, $\phi_{\beta 2}$, and ϕ_k represent the angles that the projections of these vectors on the xy plane, make with the x direction. Then,

$$\boldsymbol{Q}_1 \cdot \boldsymbol{r}_{\beta 2} = Q_1\, r_{\beta 2}\, F_{\beta 2}\left(\theta_1, \phi_1\right)$$

where, Q_1 and $r_{\beta 2}$ represent the magnitudes of $\boldsymbol{Q}_1$ and $\boldsymbol{r}_{\beta 2}$, respectively, and,

$$F_{\beta 2}\left(\theta_1, \phi_1\right) = \sin\theta_1 \sin\theta_{\beta 2} (\cos\phi_1 \cos\phi_{\beta 2} + \sin\phi_1 \sin\phi_{\beta 2}) + \cos\theta_1 \cos\theta_{\beta 2}$$

Defining the function $F_k\left(\theta_1, \phi_1\right)$ similarly, we can rewrite the $\boldsymbol{Q}_1$ integral in expression (100), in terms of spherical coordinates as,

$$I_{Q_1} = \int_0^\infty dQ_1 \int_0^{2\pi} d\theta_1 \int_0^\pi d\phi_1\, Q_1^2\, \sin\theta_1\, \exp\left[-\frac{H}{2k_{\rm B}T}\, Q_1^2 - i\,\delta_{1\mu}\, Q_1 k\, F_k\left(\theta_1, \phi_1\right) \right] \times$$

$$\exp\left\{-\frac{1}{k_{\rm B}T}\left[\frac{v\,k_{\rm B}T}{\left(2\pi\tilde{d}^2\right)^{3/2}}\left\{e^{-\frac{1}{2\tilde{d}^2}\,Q_1^2}+e^{-\frac{1}{2\tilde{d}^2}\left(Q_1^2+2\,Q_1\,r_{32}\,F_{32}(\theta_1,\phi_1)\right)}\,e^{-\frac{1}{2\tilde{d}^2}\,\boldsymbol{Q}_2^2}\right.\right.\right.$$
$$\left.\left.\left.+\ldots+e^{-\frac{1}{2\tilde{d}^2}\left(Q_1^2+2\,Q_1\,r_{N2}\,F_{N2}(\theta_1,\phi_1)\right)}\,e^{-\frac{1}{2\tilde{d}^2}\left(\boldsymbol{Q}_2^2+2\,\boldsymbol{Q}_2\cdot\boldsymbol{r}_{N3}+\ldots+\boldsymbol{Q}_{N-1}^2\right)}\right\}\right]\right\} \tag{101}$$

For $Q_1 = 0$, the integrand is identically zero. For $Q_1 \neq 0$, in the limit $\tilde{d} \to 0$ or $\tilde{d} \to \infty$, the integrand tends to,

$$Q_1^2\,\sin\theta_1\,\exp\left\{-\frac{H}{2k_{\rm B}T}\,Q_1^2 - i\,\delta_{1\mu}\,Q_1 k\,F_k\left(\theta_1,\phi_1\right)\right\}$$

The integrand is also a bounded function of Q_1 for all values $\tilde{d}$.

An argument similar to the one above can be carried out for each of the remaining integrations over $\boldsymbol{Q}_2,\ldots,\boldsymbol{Q}_{N-1}$. It follows that,

$$\lim_{\substack{\tilde{d}\to 0\\ \text{or, } \tilde{d}\to\infty}} \int d\boldsymbol{Q}_1\ldots d\boldsymbol{Q}_{N-1}\,\exp\left\{-\left(\frac{\phi}{k_{\rm B}T}\right) - i\left(\sum_{j=\mu}^{\nu-1}\boldsymbol{Q}_j\right)\cdot\boldsymbol{k}\right\}$$
$$= \int d\boldsymbol{Q}_1\ldots d\boldsymbol{Q}_{N-1}\,\exp\left\{-\left(\frac{H}{2k_{\rm B}T}\right)\sum_{j=1}^{N-1}\boldsymbol{Q}_j^2 - i\left(\sum_{j=\mu}^{\nu-1}\boldsymbol{Q}_j\right)\cdot\boldsymbol{k}\right\} \tag{102}$$

With regard to the normalization factor $\mathcal{N}_{\rm eq}$, since,

$$\mathcal{N}_{\rm eq} = \left[\int d\boldsymbol{Q}_1\ldots d\boldsymbol{Q}_{N-1}\,\exp\left(-\frac{\phi}{k_{\rm B}T}\right)\right]^{-1} \tag{103}$$

we can show, by adopting a procedure similar to that above that,

$$\lim_{\substack{\tilde{d}\to 0\\ \text{or, } \tilde{d}\to\infty}} \mathcal{N}_{\rm eq} = \mathcal{N}_{\rm eq}^R \tag{104}$$

As a result,

$$\lim_{\substack{\tilde{d}\to 0\\ \text{or, } \tilde{d}\to\infty}} P_{\rm eq}(\boldsymbol{r}_{\nu\mu}) = \frac{1}{(2\pi)^3}\int d\boldsymbol{k}\,e^{i\,\boldsymbol{r}_{\nu\mu}\cdot\boldsymbol{k}}\left\{\int d\boldsymbol{Q}_1\ldots d\boldsymbol{Q}_{N-1}\,\psi_{\rm eq}^R\,e^{-i\left[\sum_{j=\mu}^{\nu-1}\boldsymbol{Q}_j\right]\cdot\boldsymbol{k}}\right\}$$
$$= P_{\rm eq}^R(\boldsymbol{r}_{\nu\mu}) \tag{105}$$